

Article

Classification of Land Cover, Forest, and Tree Species Classes with ZiYuan-3 Multispectral and Stereo Data

Zhuli Xie ^{1,2}, Yaoliang Chen ^{3,4}, Dengsheng Lu ^{1,2,*}, Guiying Li ^{3,4}  and Erxue Chen ⁵

¹ State Key Laboratory of Subtropical Silviculture, Zhejiang A&F University, Hangzhou 311300, China; xiezhuli_1@163.com

² School of Environmental & Resource Sciences, Zhejiang A&F University, Hangzhou 311300, China

³ State Key Laboratory for Subtropical Mountain Ecology of the Ministry of Science and Technology and Fujian Province, Fujian Normal University, Fuzhou 350007, China; chenyl@fjnu.edu.cn (Y.C.); ligy326@yahoo.com (G.L.)

⁴ School of Geographical Sciences, Fujian Normal University, Fuzhou 350007, China

⁵ Institute of Forest Resources Information Technique, Chinese Academy of Forestry, Beijing 100091, China; chenerx@ifrit.ac.cn

* Correspondence: luds@zafu.edu.cn; Tel./Fax: +86-571-6374-6366

Received: 6 November 2018; Accepted: 12 January 2019; Published: 16 January 2019



Abstract: The global availability of high spatial resolution images makes mapping tree species distribution possible for better management of forest resources. Previous research mainly focused on mapping single tree species, but information about the spatial distribution of all kinds of trees, especially plantations, is often required. This research aims to identify suitable variables and algorithms for classifying land cover, forest, and tree species. Bi-temporal ZiYuan-3 multispectral and stereo images were used. Spectral responses and textures from multispectral imagery, canopy height features from bi-temporal stereo imagery, and slope and elevation from the stereo-derived digital surface model data were examined through comparative analysis of six classification algorithms including maximum likelihood classifier (MLC), k-nearest neighbor (kNN), decision tree (DT), random forest (RF), artificial neural network (ANN), and support vector machine (SVM). The results showed that use of multiple source data—spectral bands, vegetation indices, textures, and topographic factors—considerably improved land-cover and forest classification accuracies compared to spectral bands alone, which the highest overall accuracy of 84.5% for land cover classes was from the SVM, and, of 89.2% for forest classes, was from the MLC. The combination of leaf-on and leaf-off seasonal images further improved classification accuracies by 7.8% to 15.0% for land cover classes and by 6.0% to 11.8% for forest classes compared to single season spectral image. The combination of multiple source data also improved land cover classification by 3.7% to 15.5% and forest classification by 1.0% to 12.7% compared to the spectral image alone. MLC provided better land-cover and forest classification accuracies than machine learning algorithms when spectral data alone were used. However, some machine learning approaches such as RF and SVM provided better performance than MLC when multiple data sources were used. Further addition of canopy height features into multiple source data had no or limited effects in improving land-cover or forest classification, but improved classification accuracies of some tree species such as birch and Mongolia scotch pine. Considering tree species classification, Chinese pine, Mongolia scotch pine, red pine, aspen and elm, and other broadleaf trees as having classification accuracies of over 92%, and larch and birch have relatively low accuracies of 87.3% and 84.5%. However, these high classification accuracies are from different data sources and classification algorithms, and no one classification algorithm provided the best accuracy for all tree species classes. This research implies the same data source and the classification algorithm cannot provide the best classification results for different land cover classes. It is necessary to develop a comprehensive classification procedure using an expert-based approach or hierarchical-based classification approach that can employ specific data variables and algorithm for each tree species class.

Keywords: tree species; classification; ZiYuan-3; stereo image; machine learning

1. Introduction

A substantial decrease of global forest area from unprecedented human disturbance causes a huge loss of biodiversity [1]. The expansion of plantations compensates this damage to some extent. Plantations provide some habitat needs for a subset of animal species and diverse timbers for human use. Understanding the distribution of plantations is very important in biodiversity assessment [2], forest biomass prediction [3,4], ecosystem services and biogeochemical cycling [5–7], and forest resources management [8]. China, as the largest plantation area in the world since 1999 [9], experienced a dramatic increase from nearly 47 million hectares in 1999 to nearly 70 million hectares in 2014 [10], which requires timely updates of spatial information of forest distribution. Depending on the geolocations and climate zones in China, the spatial patterns, and types of plantations vary such as rubbers in a tropical region of south China, eucalyptus in a subtropical region in east and south China, Chinese fir plantations in the subtropical region, and different kinds of pines (e.g., larch, Chinese pine, red pine) in north China. Plantations have played more and more important roles in improving economic conditions for local persons.

Remotely sensed data has long been used for land-cover mapping in large areas due to the unique characteristics of spectral, temporal, and spatial features and a digital number data format suitable for computer processing. Satellite data, such as Landsat, have been explored extensively for land cover mapping, and even individual tree species mapping, because the data are freely available and contain a broad range of suitable spectral bands [11–14]. Dong et al. [15] combined multi-temporal Landsat images and PALSAR (Phased Array type L-band Synthetic Aperture Radar) data to map rubber tree distribution in China's Hainan Province and achieved an overall accuracy of 92%. Qiao et al. [16] applied time-series normalized difference vegetation index (NDVI) images from annual Landsat images over 15 years to identify eucalyptus in Guangdong Province and obtained an accuracy of 91%. In previous research, single-date images were mostly used because of the difficulty in obtaining images of different seasons due to poor weather conditions, especially in tropical and subtropical regions [17,18]. Seasonal vegetation information has proven valuable in improving vegetation classification [19]. In the subtropical Lin'an District mountains, Xi et al. [20] used multi-temporal Landsat images to extract hickory plantations by developing subpixel indices from linear spectral mixture analysis. Because of its relatively coarse spatial resolution in Landsat, accurate mapping of plantation distribution due to a small patch size become a challenge.

In recent years, attention has shifted to using high spatial resolution satellite data for detailed classification because of its better ability to capture fine characteristics of objects [21–23]. Gomez et al. [17] used QuickBird multispectral and panchromatic images to extract coffee plantations in NewCaledonia and obtained an accuracy of 96.9%. Cho et al. [24] applied WorldView-2 images to extract three tree species in South Africa and obtained an accuracy of 89.3%. Wang and Lu [25] used the expert-rule based approach based on Chinese Gaofen (GF-1) and ZiYuan (ZY-3) satellite images to successfully map *Torriya* forest distribution with an overall accuracy of 84.4%. High spatial resolution data with multi-temporal features are especially valuable for improving vegetation classification accuracy [19]. Reis and Tasdemir [26] applied QuickBird data during the growing and deciduous seasons to identify hazelnut in northeastern Turkey and found that accuracy increased by 9% compared to using single-season data. Li et al. [19] used four-seasonal GF-1 images to map wetland classification in Hangzhou Bay, China using the expert-based approach with an overall classification accuracy of 90.3%. However, processing and analysis of high spatial resolution satellite data also pose challenges in terms of large file sizes, canopy shadows, and high spectral variation within the forested areas.

The selection of suitable variables from remotely sensed data is one of the critical steps in improving classification accuracy [27]. Since high spatial resolution data often have limited spectral

information. The incorporation of spatial-based variables into spectral features becomes critical [19,21]. Pixel-based features can be individual spectral bands, vegetation indices, or transformed images. Spatial-based features can be textural images or segmentation [27]. Many previous studies indicated that combinations of spectral and spatial features improved classification accuracy [18,28] and the object-based classifier provided better accuracy than pixel-based approaches when high spatial resolution images were used [21,23,29,30]. Dihkan et al. [31] found that overall accuracy was improved from 93.82% to 97.40% after integration of textures and multispectral images for mapping tea plantations using a support vector machine (SVM).

For forest classification, use of the forest stand structure features may support the separation of different tree species or forest types due to the difference in tree species composition, crown size and shape, and tree density [32,33]. One critical step is to extract suitable forest attributes such as canopy height and crown size. The height information was found to be useful in improving classification accuracy of tree species [34–37]. Holmgren et al. [34] compared the results of mapping tree species in southern Sweden by separately using three variable conditions (only height information from lidar, only variables from multispectral data, and a combination of height information and variables from multispectral data) and found that spectral variables combined with height information provided the highest accuracy. Ke et al. [36] also found that adding height information improved tree species mapping accuracy by 3%. In reality, use of height information in forest classification is still very limited in previous research due to the difficulty in obtaining height images in a large area, but could be an important factor in improving forest classification in the future because of the availability of lidar and satellite stereo images.

Many classifiers from statistical-based algorithms—e.g., cluster analysis [38], maximum likelihood classifier (MLC) [26]—to machine learning algorithms—e.g., decision tree (DT) [36], artificial neural networks (ANN) [17], SVM [39], expert rules-based approach [25], and random forest (RF) [37,40]—have been used for land-cover classification based on high spatial resolution imagery. Previous research implies that the choice of the best classifiers depends mainly on the specific study area, data, and land-cover classification system [19,27]. Raczko and Zagajewski [41] compared three machine learning classifiers in identifying five tree species and found that ANN achieved the highest accuracy. Li et al. [19] applied MLC, RF, and the expert rules-based approach to classify nine land-cover classes from four seasons of GF-1 multispectral images in Hangzhou Bay coastal wetland. An accuracy of 90.3% was obtained using the expert rules-based approach. Recent research explored the use of deep learning in tree species mapping [42–44]. However, more investigation is needed for this method since it is highly complex and is computationally intensive.

Forest inventories at the county or forest farm scale in China in the 1980s and 1990s were usually conducted at 10-year intervals using field surveys, topographic maps, and aerial photographs to create detailed forest distribution maps of tree species, especially for plantations, and to make plans for forest management. Entering the 2000s, as high spatial resolution satellite images such as QuickBird, SPOT, and WorldView became widely available, forest inventory was mainly based on visual interpretation of the images with support from field surveys. Because these processes were time consuming and labor intensive, and updating and incorporating data from previous inventories was difficult, research in recent years has shifted to computer-based automatic classification based on the satellite images. Although the important role of using high spatial resolution images in improving the quality of mapping forest distribution has been recognized, they have not been extensively used in real applications. Three major reasons may account for this: (1) the difficulty of using automatic classification of forest types within existing classification approaches, (2) the limitation of spectral wavelengths (usually only visible and NIR bands) resulting in the challenge of separation of tree species, and (3) the costs of image purchase, purchase of computers that can deal with large volumes of data, and hiring data-processing professionals. However, high spatial resolution data will play an increasingly important role in the future, for producing detailed forest classification and conducting forest inventory at local and regional scales.

Although many studies explored tree species classification using high spatial resolution images, they mainly focused on single tree species without taking multiple tree species into account. Many variables from spectral signatures, vegetation indices, texture, and ancillary data can be used for tree species classification. However, not all variables are needed and improper combinations of different variables may yield poor classification results. Overfitting in the machine learning algorithms is also a problem. To date, it is still unclear which classification algorithm provides the best performance and how different seasonal features, and different data sources influence land cover or forest classification. The objectives of this research are to explore (1) the incorporation of different seasonal data (leaf-on, leaf-off), (2) combination of different kinds of variables (spectral, vegetation indices, textures, shape variables, topographic factors, and height features), and (3) different classifiers (MLC, ANN, k-nearest neighbor (kNN), DT, RF, and SVM) in improving land cover (all forest and non-forest classes), forest (all tree species classes), and tree species mapping performance. Therefore, high spatial resolution multi-spectral and panchromatic data, satellite stereo images, and topographic data were selected in a plantation-dominated study area in north China. The contribution of this research is to identify the best classification procedures for land cover, forest, and tree species classification using high spatial resolution images through comparative analysis of the classification results based on different scenarios. Other contributions include the calculation of textural images based on segmented polygons instead of traditional approaches based on fixed window sizes and the use of canopy height features in improving forest and tree species classification accuracies. This research will provide new insights on how to select suitable variables and classification algorithms for land cover and forest classification, especially in temperate monsoon climate regions.

2. Materials and Methods

2.1. Study Area

In order to explore the classification performance using different data sources and classification algorithms, selection of a typical study area is important. Wangyedian Forest Farm with a total area of approximately 500 km², which is located in southwestern Kelaqin, Inner Mongolia, China, was an ideal study area because of its spatial distribution of typical coniferous forest plantations in a temperate climate zone (Figure 1). Plantation types mainly include four needle forests (larch, Chinese pine, Mongolia scotch pine, and red pine) and three deciduous broadleaf forests (birch, aspen, and elm) [45]. Aspen and elm are mainly distributed along roads and around villages, while birch is in the mountainous areas. This study area is located at relatively high elevations of 1810 m in the west and 783 m in the east (Figure 1). The region has a typical middle continental temperate monsoon climate with four seasons: dry with frequent wind in the spring, wet and hot in the summer, frequent frosts in the fall, and cold with a little snow in the winter [46]. Average annual temperatures range from 3.5 °C to 7 °C and average annual rainfall is around 400 mm [47].

Founded in 1956 and managed by the former State Forestry Administration until 1978, this farm was administratively incorporated to Chifeng City. Because it is a state property, management has focused on afforestation, and harvesting has been strictly prohibited. In 1956, this forest farm had natural forest areas of about 7300 ha [48]. Between 1956 and 1990, about 15,300 ha of man-made forests were planted, and, between 1991 and 2006, the emphasis was on the intensive forest management for the young and middle-age plantations in order to improve the forest quality. After 2007, harvesting of natural forests was prohibited. By 2014, the forested area was over 22,000 ha, with plantations accounting for almost half of it [49].

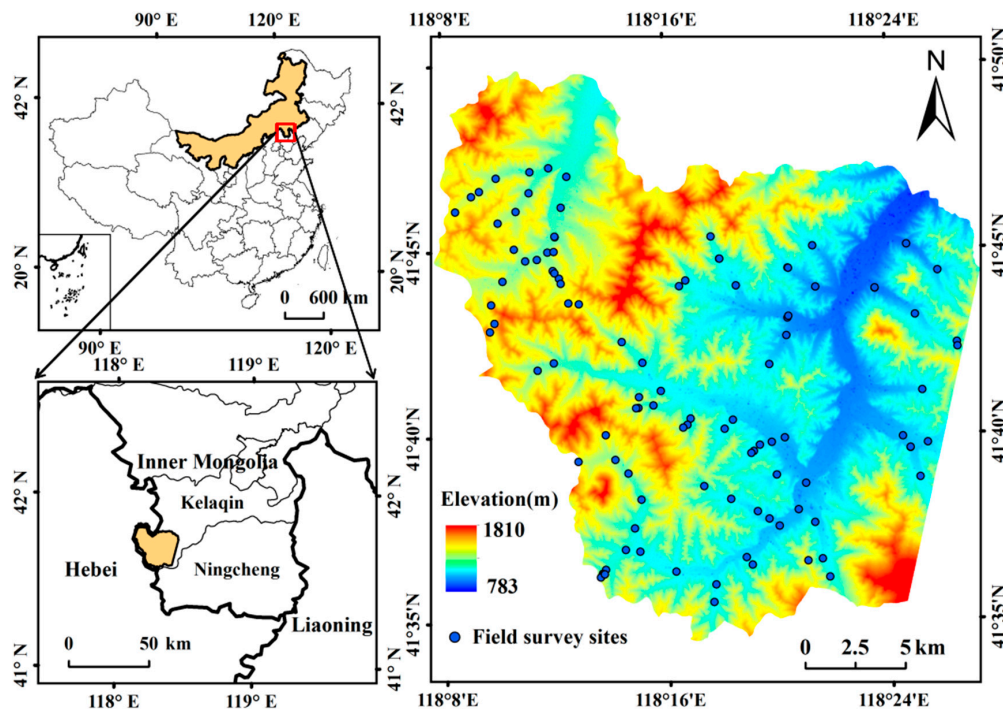


Figure 1. Study area: Wangyedian Forest Farm in eastern Inner Mongolia, China.

2.2. Data Preparation

2.2.1. Field Survey Data Collection

Datasets used in this study include field survey data and ZiYuan (ZY-3) multispectral, panchromatic, and stereo data (Table 1). We first designed the sites for the field survey based on the high spatial resolution image and previous forest map in this study area. During the field work, we recorded all land cover types around each site. We then digitized all recorded land cover types on the google earth image and formed a shape file format file. The land covers recorded include larch, Chinese pine (CP), Mongolia scotch pine (MSP), red pine (RP), birch, aspen, elm, other broadleaf tree species (OBL), shrub, grass, farmland (FL), bare land (BL), impervious surface area (ISA), and water. Based on our research objectives and consideration of the separability of land-cover types, a classification system with 13 land-cover types including seven tree species (larch, CP, MSP, RP, birch, aspen, and elm (AAE), OBL) designated as forest, and shrub, grass, FL, BL, ISA, and water—were defined. According to this classification system, the classification results were analyzed on three levels—land cover (all 13 classes), forest (all seven tree species classes), and tree species (each tree species class).

Table 1. Data used in the research.

Data	Data Description	Data Acquisition Dates
Field survey data	A total of 112 sites were investigated, for which all land covers around each site were recorded, digitized, and saved in a shape file format. Thus, over 1000 samples covering different land covers were collected.	September 2017
ZiYuan-3 satellite data	Four multispectral bands (blue, green, red, and near infrared (NIR)): 5.8 m spatial resolution; One panchromatic band: 2 m spatial resolution; Stereo images: nadir-view image with 2 m, backward and forward views with 3.5 m spatial resolution	9 February 2015: sun elevation angle of 31.44° and azimuth angle of 163.06°; 20 September 2017: sun elevation angle of 44.22° and azimuth angle of 148.18°

2.2.2. ZiYuan-3 Satellite Data Collection and Pre-Processing

Because of the good data quality, high spatial resolution, and the availability of multi-spectral and stereo data (Table 1), ZY-3 satellite data are increasingly used in land-cover classification [50–52]. Ideally, different seasonal images in a year will be valuable for mapping forest distribution. After we

searched all images within three years, we find only two cloud-free images that were acquired in leaf-on and leaf-off season each, but they were not from the same year. Therefore, two scenes of ZY-3 images, which were acquired on 27 September, 2017 (leaf-on season) and on 9 February, 2015 (leaf-off season) were used. Figure 2 shows different representations of four kinds of tree species classes on leaf-on and leaf-off ZY-3 color composites. The ZY-3 stereo images from the same dates were used to produce digital surface model (DSM) data for this study area. In order to convert digital number data to surface reflectance in the ZY-3 multispectral images, the dark-object subtraction approach [53] was used for atmospheric calibration. Because previous research showed that the C-correction model [54,55] is suitable for images with steep slope terrains and low sun zenith angle [56], we used this method for topographic correction. In order to make full use of different features in multi-spectral and panchromatic data, it is necessary to identify suitable data fusion algorithms to conduct this data fusion. The Gram-Schmidt tool is regarded as a good fusion technique that can improve spatial information while minimizing spectral distortion [57,58]. Thus, this method was used to integrate multi-spectral and panchromatic data to produce a new dataset with a spatial resolution of 2 m.

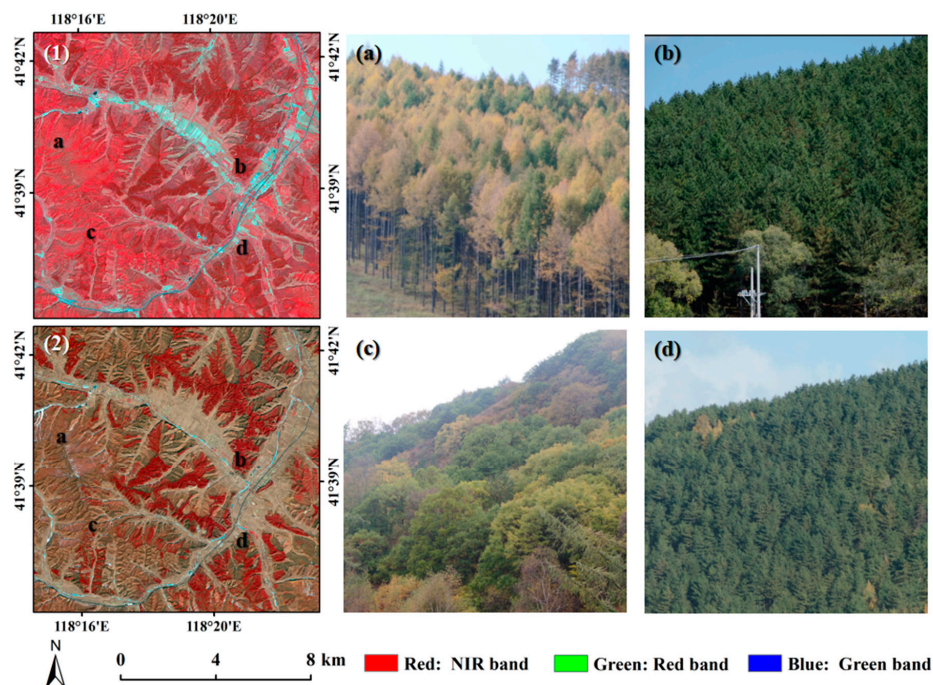


Figure 2. A comparison of color composites in leaf-on season (1) and leaf-off season (2) showing different representations of four tree species classes: birch (a) Chinese pine (b) a composite of different broadleaf tree species (c) and larch (d).

2.2.3. Development of Digital Surface Model Data from Stereo Images

The digital elevation model (DEM) data with high spatial resolution are needed for topographic correction in this research. However, this kind of data is not available. Thus, we developed DSM data from ZY-3 stereo images using the Geomatica PCI software with the following steps: (1) Relative orientation was conducted to create a surface three-dimensional model. The rational polynomial coefficients (RPC) parameter file was used to locate the relative position between two different views [59]. (2) Absolute orientation was then conducted to fix the geometric location of a three-dimensional model in the ground measurement coordinate system by translating, rotating, and scaling based on selected ground control points (GCPs) [60,61]. (3) Tie points connecting two images were created to establish a relationship between them. An initial DSM was subsequently established as well as the errors of tie points and GCPs. If the error was too large, we eliminated tie points with large errors and recalculated the model. (4) An epi-polar image was developed and

its corresponding DSM was extracted [62]. Two combinations of views—nadir and backward views, nadir and forward views—were used to extract the DSM. In order to test the accuracy of the extracted DSM, 65 points with flat topography (e.g., at a crossroad and in the farmland area) were selected from Google Earth maps. Results showed that the mean errors in the DSM at leaf-on and leaf-off seasons were 4.47 and 3.75 m, respectively. The DSM data at the leaf-on season were used for topographic correction. The DSM data from the leaf-off season were not used for topographic correction due to the different impacts of deciduous and evergreen forests on DSM data.

Previous research used both DSM images from the leaf-on and leaf-off seasons to produce a canopy height image [59]. However, for this research, we called this kind of differencing image as relative canopy height (RCH), considering the different effects of deciduous and evergreen forests. For deciduous forests, the difference of both DSMs from leaf-on and leaf-off seasons can be assumed as the canopy height. However, for the evergreen forests, the differencing image cannot represent the canopy height. Figure 3 shows the developed DSM images from leaf-on and leaf-off seasons, as well as the RCH image (Figure 3C) from the difference of both DSM images. As a comparison, we also included a color composite (Figure 3D) using the ZY-3 multi-spectral image at leaf-on season at the same site and added some specific forest types (e.g., a: birch, b: Mongolia scotch pine, c: other broadleaf, d: Chinese pine, and e: larch) to show the impacts of deciduous and evergreen forest types on the RCH values. Although the RCH image cannot represent the real canopy height values of different forest types, Figure 3 indicates that proper use of this feature may be helpful for improving forest classification or forest and non-forest separation.

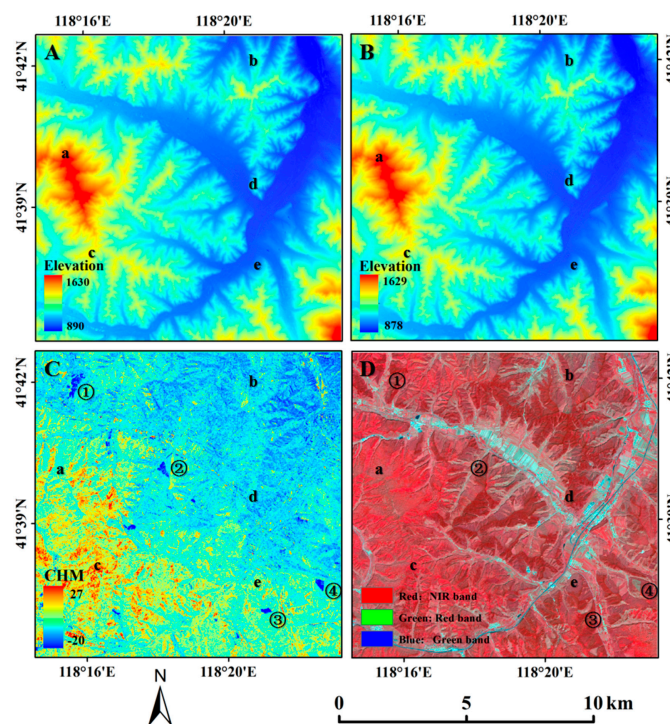


Figure 3. A comparison of the digital surface model (DSM) images from leaf-on season (A) and leaf-off season (B). The difference between DSMs was used to produce a relative canopy height (RCH) image, especially for a deciduous forest (C). As a comparison with the RCH image, a color composite (D) using the ZiYuan-3 multispectral image at the leaf-on season at the same site was provided (a: birch, b: Mongolia scotch pine, c: other broadleaf, d: Chinese pine, and e: larch). The blue color in locations ①, ②, ③, and ④ indicates deforestation sites of plantations between 2015 and 2017.

2.2.4. Development of the Segment Image

Previous research shows that the object-based classification approach provided better land cover accuracy than pixel-based approaches when high spatial resolution images were used [19,21,23]. Pixel-based approaches classify each pixel into only one class based on the digital value of each pixel, and are very commonly used, especially when medium spatial resolution images such as Landsat were used [27,63,64]. However, pixel-based approach may produce poor classification results when very high spatial resolution images are used because of high spectral variation within the same land cover type [21,22]. In the object-based approach, one critical step is to develop a suitable segment image. In our research, we used the eCognition software, in which four key parameters—weight of input layers, weight of spectra and shape, weight of compacts and smoothness, and scale of segment—need to be carefully defined in the segmentation procedure. Generally, the sum of spectra, shape weights, sum of compact, and smoothness should be 1. In this study, shape weight and compact weight were set as 0.2 and 0.5, respectively, after a substantial number of adjustments. The scale of the segment also needs to be optimized by continuously checking the segment result and setting it as 100. According to the optimization, if the scale is too large, aspen, elm, and grass cannot be separated well. In contrast, if the scale is too small, the segmented polygons will be too fragmented. Based on the developed segment image, all variables such as vegetation indices and textures were extracted, according to this segment image.

2.2.5. Framework of This Research

The framework of the mapping land cover, forest, and tree species distribution using ZY-3 data is illustrated in Figure 4. This framework includes five major steps: (1) data collection and preprocessing, (2) extraction and identification of variables from ZY-3 data, (3) selection of suitable classifiers, (4) design of classification scenarios and implementation of image classification corresponding to each scenario, and (5) validation of classification results.

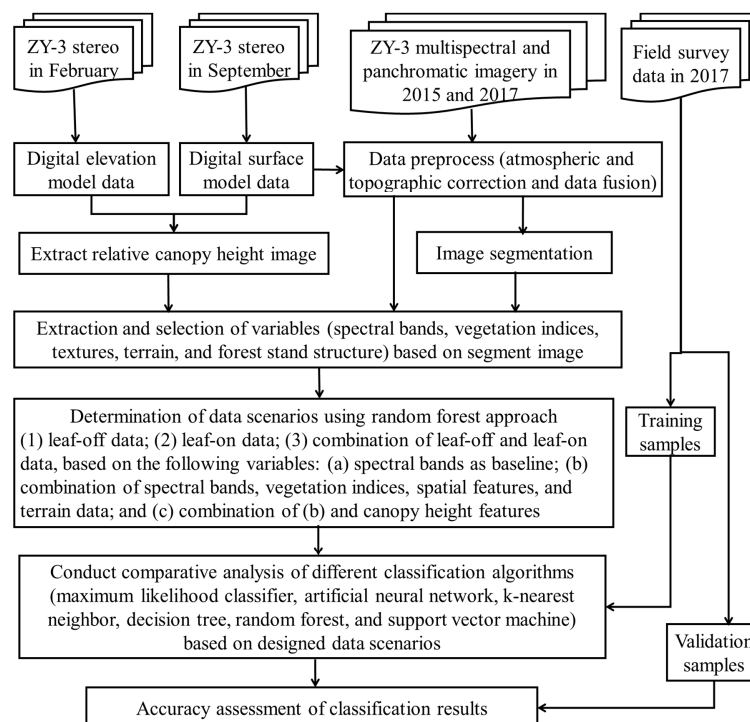


Figure 4. Framework of mapping land cover, forest, and tree species distribution through a comparative analysis of classification results using different classification algorithms based on various scenarios from ZiYuan-3 (ZY-3) data.

2.3. Extraction of Potential Variables and Selection of Optimal Variable Combination

In remote sensing optical sensor data, the spectral, spatial, temporal, and subpixel features are extensively used for land-cover classification [26]. In this research, five kinds of features were considered: (1) pixel-based spectral features such as spectral signatures and vegetation indices, (2) spatial-based features such as textural images and image segmentation, (3) temporal features such as growing and deciduous seasons, (4) height-based variables that can reflect the difference of forest stand structures, and (5) topographic factors such as slope and elevation.

2.3.1. Extraction of Spectral-Based Variables

Spectral data—spectral bands, vegetation indices, and transformed images—are commonly used for land-cover classification [27]. In this research, spectral data include four original bands (blue, green, red, and NIR), the sum of four bands, ratio of each band to the sum of four bands, and different vegetation indices, which are summarized in Table 2. In order to use temporal information, differences between specific bands of bi-temporal images and differences between vegetation indices (VDVI(diff) and NDGI(diff), respectively) were also used.

Table 2. Vegetation indices used in this research.

Vegetation Indices	Equations	References
Differenced vegetation index (DVI)	$NIR - Red$	[65]
Infrared percentage vegetation index (IPVI)	$NIR / (NIR + Red)$	[66]
Normalized difference vegetation index (NDVI)	$(NIR - Red) / (NIR + Red)$	[65]
Normalized difference greenness index (NDGI)	$(Green - Red) / (Green + Red)$	[65]
Normalized difference water index (NDWI)	$(Green - NIR) / (Green + NIR)$	[65]
Ratio vegetation index (RVI)	NIR / Red	[25]
Re-normalized difference vegetation index (RDVI)	$(NIR - Red) / \sqrt{(NIR + Red)}$	[4]
Visible-band difference vegetation index (VDVI)	$\frac{((Green - Red) + (Green - Blue))}{(Green + Red + Green + Blue)}$	[67,68]
Optimized soil adjusted vegetation index (OSAVI)	$(NIR - Red) / (NIR + Red + 0.16)$	[4]
Ratio of near-infrared (NIR) band to blue band	$NIR / Blue$	[25]

2.3.2. Extraction of Spatial-Based Variables

Spatial features are important for high spatial resolution images and are used for land-cover classification [23,27]. Common spatial features are textures and segmentation. Traditionally, textures are calculated with a fixed window size (e.g., 3×3 , 5×5) based on a spectral band. However, because of the difference in patch sizes among land-cover types and locations, it is difficult to identify optimal textural images that are suitable for different land covers [28]. In order to avoid this problem that no one optimal window size is available for different patch sizes of land covers, we calculated textural images based on the segmented objects using the gray-level co-occurrence matrix (GLCM) measures. Eight texture measures (mean, standard deviation, homogeneity, contrast, dissimilarity, entropy, second moment, and correlation) [69] were calculated in this research. Another important spatial feature is based on the segmented polygons, including length, width, area, ellipse, rectangle, shape index, brightness, and border index that they are directly provided from the segmented results using eCognition software [70,71].

2.3.3. Extraction of Forest Stand Based Variables

Different tree species have their own crown sizes, canopy density, and vertical structure. Effective use of forest stand structure features is regarded as an important approach to improve tree species or forest type separation [33]. In this research, an RCH image was extracted from the difference of DSM data between leaf-on and leaf-off seasons based on the assumption that leaf-on DSM represents canopy height and leaf-off DSM represents ground elevation [59]. From the RCH image (see Figure 3(3)), the variables reflecting the difference of forest stand features were then extracted using the GLCM measures based on the segmented polygons.

2.3.4. Extraction of Topographical-Based Variables

Topography is related to tree species distribution and topographic factors such as elevation, slope, and aspect, which are often used to support forest classification [27]. This research selected leaf-on DSM data from ZY-3 stereo images for calculation of slope, aspect, and elevation. These factors were used as extra variables by combining them with remote sensing variables for land-cover classification.

2.3.5. Selection of Suitable Variables Using Random Forest

Although many variables can be extracted, they are not all needed for land-cover or forest classification. The best combination of variables must be identified. Thus, the RF approach was used because it can provide rankings of variable importance [4]. The selection of variables using the RF approach was conducted using R software. For each decision tree of RF, the out-of-bag (OOB) error was calculated (errOOB1) and random noise was added into a certain variable X of OOB from all samples (errOOB2). The importance of variable X is assumed as the mean value of the sum of differences between errOOB2 and errOOB1 in all trees. If variable X has a great influence on the classification result, the OOB accuracy will be considerably reduced after adding random noise, which indicates its high importance [70]. Pearson’s correlation analysis of the selected variables using RF was conducted after the importance ranking. For two variables having a correlation coefficient of greater than 0.8, the one having lower importance ranking was removed if removal of this variable did not produce a higher error in the RF procedure. All variables were checked during this process, and the selected variables were not highly correlated to one another.

Table 3 summarized the selected variables using RF based on different data scenarios—leaf-off, leaf-on, and the combination of those seasons. V1off, V1on, and V1both represent the spectral bands only at leaf-off, leaf-on, and combination of both seasons. The selected variables in V2off, V2on, and V2both included spectral responses (spectral band or vegetation index), textural images, and topographic factors, which implies the importance of using multiple source data in land-cover classification. Considering scenario V3, three and two forest stand variables corresponding to V3off and V3on and one forest stand variable corresponding to V3both were selected, which implies that forest stand structure may be useful in improving land-cover, especially tree species classification.

Table 3. Selected variables for use in land-cover classification.

Data	Variables
Data from leaf-off season	V1off Blue _F , Green _F , Red _F , NIR _F .
	V2off NDVI _F , Brightness, NDGI _F , Slope, NIR _F , Elevation, T _{F-Cor-NIR} , T _{F-Cor-Green} , VDVI _F , Aspect, T _{F-Hom-Red} , T _{F-Hom-Blue} , T _{F-Std-Red} .
	V3off NDVI _F , RCH, Brightness, NDGI _F , Slope, NIR _F , Elevation, T _{F-Cor-NIR} , T _{F-Cor-Green} , VDVI _F , T _{Ent-RCH} , Aspect, T _{F-Hom-Red} , T _{Dis-RCH} , T _{F-Hom-Blue} , T _{F-Std-Red} .
Data from leaf-on season	V1on Blue _S , Green _S , Red _S , NIR _S .
	V2on SUM _{S-all-band} , VDVI _S , T _{S-Sec-Blue} , NIR/SUM _{S-all-band} , NIR/BLUE _S , NIR _S , Elevation, T _{S-Std-Red} , T _{S-Hom-NIR} , NDGI _S , Slope, T _{S-Dis-NIR} , T _{S-Con-Red} , T _{S-Ent-NIR} , Length/Width.
	V3on SUM _{S-all-band} , VDVI _S , T _{S-Sec-Blue} , NIR/SUM _{S-all-band} , NIR/BLUE _S , NIR _S , Elevation, T _{S-Std-Red} , T _{S-Hom-NIR} , RCH, NDGI _S , Slope, T _{S-Dis-NIR} , T _{S-Con-Red} , T _{S-RCH} , T _{S-Ent-NIR} , Length/Width.
Combined data from both seasons	V1both Blue _F , Green _F , Red _F , NIR _F , Blue _S , Green _S , Red _S , NIR _S .
	V2both IPVI _F , SUM _{S-all-band} , IPVI _S , VDVI _S , NIR _S , T _{S-Sec-Blue} , NDGI (diff), NDGI _S , T _{S-Hom-NIR} , VDVI (diff), Slope, T _{S-Ent-Blue} , VDVI _F , Elevation, T _{S-Cor-Red} , NDGI _F , T _{S-Std-NIR} .
	V3both IPVI _F , SUM _{S-all-band} , IPVI _S , VDVI _S , NIR _S , T _{S-Sec-Blue} , NDGI (diff), NDGI _S , RCH, T _{S-Hom-NIR} , VDVI (diff), Slope, T _{S-Ent-Blue} , VDVI _F , Elevation, T _{S-Cor-Red} , NDGI _F , T _{S-Std-NIR} .

Note: F, ZiYuan-3 multispectral data in February, NIR, near infrared, NDVI, normalized difference vegetation index, NDGI, normalized difference greenness index, T, texture, VDVI, visible-band difference vegetation index, RCH, relative canopy height, S, ZiYuan-3 multispectral data in September, IPVI, infrared percentage vegetation index, different texture measures: Cor, correlation, Ent, entropy, Hom, homogeneity, Dis, dissimilarity, Std, standard deviation, Sec, second moment, Con, contrast, different vegetation indices: NDVI = (NIR-Red)/(NIR + Red), NDGI = (Green-Red)/(Green + Red), VDVI = ((Green-Red) + (Green-Blue))/(Green + Red + Green + Blue), IPVI = NIR/(NIR + Red), NDGI(diff) = NDGI_S-NDGI_F, VDVI(diff) = VDVI_S-VDVI_F.

2.4. Comparative Analysis of Classification Algorithms

2.4.1. A Brief Description of Six Classification Approaches

Although many classification approaches are available, the one that can provide the best classification result for a specific study area is unclear. In reality, several classifiers are often selected for a comparative analysis of the results [63,64]. In this research, six classifiers—maximum likelihood classifier (MLC), k-nearest neighbor (kNN), decision tree (DT), random forest (RF), artificial neural network (ANN), and support vector machine (SVM)—were selected. Three classifiers—MLC, SVM, and ANN—were conducted using ENVI, and another three—DT, RF, and kNN—were conducted using Weka. MLC is a traditional and widely used classifier in remote sensing classification applications [3,27,72]. This method calculates probabilities of each pixel that belongs to each land-cover type by a determining function deduced from training samples [73]. Thus, the land-cover type of a pixel is determined as the one with the highest probability. This method is simple to apply and can produce a classification map quickly, but it relies heavily on the representative of training samples for each class and requires that values of the selected variables have a normal distribution for each land cover class [74].

ANN is a machine learning algorithm in the field of artificial intelligence. Neural network is a computing model composed of substantial nodes, including the input layer, hidden layer, and output layer [75]. In this algorithm, the output layer of a previous node could be the input layer of the next node and the output of the network varies for different connecting styles, weight values, and incentive functions. Thus, this method is capable of parallel computing, automatically learning, and correcting errors. However, the learning is slow and the process cannot be observed. The major parameters of ANN include training rate, training momentum, training RMSE (root mean square error) exit criteria, and the number of training iterations. Detailed parameter settings can be found in Gong et al. [76]. Note that the number of training iterations should not be too large or too small. In this study, it was set at 1000.

The main idea of kNN is that, if the testing object and k of its neighborhood objects in feature space all belong to a sample land-cover type, the object belongs to this land-cover type. This method is simple and effective, and is appropriate for those samples that cross multiple classes [77]. Similar to MLC, kNN can be highly affected by the representatives of training samples for each class. The determination of k 's value is important in this method. If k is too small, the results will be largely affected by noise. In contrast, if k is too large, the boundaries of different classes could be blurred [78–80]. In this study, k was optimized by an iterated cross-validation.

The core structure in DT is a tree structure with many nodes. Each node represents a testing of a variable, and each branch represents a testing output. Each leaf node represents an output class [81–83]. Branch pruning is an intermediate process in DT and can largely affect the final classification result. Two kinds of branch pruning—pre-pruning and post-pruning—are provided. The former will pre-set a threshold before a tree grows. Once the threshold is achieved, the growing will stop and the stopping nodes become leaf nodes. Thus, the threshold is very important and, if it is not set well, the result will be inadequate. In contrast, post-pruning will let the tree fully grow until all the leaf nodes have the smallest impurity [84]. Previous research suggests that post-pruning is better than pre-pruning for a small number of samples [85]. For a large number of samples, post-pruning needs much more computation than pre-pruning. Thus, the trade-off between efficiency and accuracy should be carefully considered before selecting the pruning method. In this study, post-pruning was used considering the relatively small number of samples. Overall, DT is simple and easy to understand but also accumulates the commission errors for the deep branches and tends to over-fit the final mapping result [86,87].

RF contains multiple decision trees. The final classification result is determined by a voting process of all the trees. RF includes two kinds of random selection. One is the training dataset. It randomly creates many subsets from a training dataset. Each subset corresponds to a subtree and a classification result. Thus, the final output is determined by the voting results from all subtrees [88]. Another is the

random selection of variables. Similar to randomly selecting data, the optimal variables are voted by all the randomly selected sub-variables used in the tree nodes [89]. Overall, RF can tackle complex data with large dimensions and can output the importance ranking of all variables. The disadvantage of this method is that classification is likely to over-fit the final results [90].

SVM is increasingly applied for land-cover classification because of its capability to solve problems with a small number of training samples and nonlinearity [91]. However, it is very sensitive to a lack of data [73,92]. SVM provides four kinds of core models (linear, polynomial, radial basis function (RBF), and sigmoid) [93,94]. In this study, RBF was selected after comparing classification results of the four types. Parameters of RBF include gamma in kernel function, penalty parameter, and probability threshold. The two former parameters were optimized by comparing the classification results after continuously adjusting them. The probability threshold ranges from 0 to 1. Pixels with probability smaller than this threshold will not be classified. Thus, thresholds were set at zero to avoid unclassified pixels in this study.

2.4.2. Comparative Analysis of Classification Results

In order to examine the roles of different data scenarios and classification algorithms in land-cover or forest mapping performance, we designed a total of 54 scenarios comprised of three datasets (leaf-on, leaf-off, and their combination), three categories of variables (V1: spectra bands, V2: V1 plus texture, vegetation indices, segmented shapes indices, and topographic variables, V3: V2 plus RCH features), and six classifiers (MLC, ANN, kNN, DT, RF, and SVM). Based on field survey data and Google Earth imagery, the numbers of training and validation samples were selected and summarized in Table 4.

Table 4. Summary of samples for training and validation for each land cover class.

Samples	Number of Samples for Each Class													Total
	Larch	CP	MSP	RP	Birch	AAE	OBL	Shrub	Grass	FL	BL	Water	ISA	
Training	167	221	36	16	83	69	71	33	45	105	48	14	148	1056
Validation	58	95	31	30	59	43	52	53	68	85	47	30	31	682

Note: CP: Chinese pine, MSP: Mongolia Scotch pine, RP: red pine, AAE: aspen and elm, OBL: other broadleaf tree species, FL: farmland, BL: bare land, ISA: impervious surface area.

Traditionally, the error matrix is used to evaluate classification accuracy. From the error matrix, user's accuracy and producer's accuracy are calculated for the evaluation of individual classes, and overall accuracy and kappa coefficients are used to evaluate the overall classification performance [95,96]. In addition, other approaches as summarized by Liu et al. [97] can be used for classification accuracy assessment. In this research, the objective is to identify whether addition of variables from multiple data sources can improve classification accuracy, or which classification algorithm has better performance. Therefore, the traditional approach including overall land-cover accuracy and overall forest classification accuracy (OFCA) based on the error matrix was used. Meanwhile, tree species mapping accuracy (TSMA) based on user's and producer's accuracies was used for evaluating the accuracy of tree species classes [80]. OFCA and TSMA are expressed by the equation below.

$$OFCA = \frac{\sum_{i=1}^n TSMA_i}{n} \text{ and } TSMA_i = \frac{PA_i + UA_i}{2}, \quad (1)$$

where PA_i and UA_i are the producer's and user's accuracies, respectively, of the i th tree species type, and n is the total number of tree species types.

3. Results

3.1. Comparative Analysis of Classification Results Based on Overall Land-Cover and Forest Types

3.1.1. Classification Results Based on Overall Land Cover Classes

According to the summary of overall land-cover classification accuracy assessment results among six classification algorithms using different data sources (Table 5), the best overall accuracy of 84.5% was obtained using SVM based on the combination of spectral response (spectral bands, vegetation indices), textures, and topographic factors in both seasonal images (i.e., V2both). Considering different data sources, incorporation of spectral responses (spectral bands, vegetation indices), textures, and topographic factors (V2off) improved classification accuracy by 5.2% to 27.0% compared to spectral bands only (V1off), but further addition of RCH features into V2off (i.e., V3off) yields a slight improvement, except in kNN.

Table 5. Summary of overall accuracies of all land-cover classes among six classification algorithms based on different data sources.

Data Scenarios		Overall Land-Cover Classification Accuracy (%) Based on Six Algorithms					
		MLC	ANN	kNN	DT	RF	SVM
Data from leaf-off season	V1off	68.62	41.64	48.97	50.29	57.92	57.18
	V2off	76.10	45.45	75.95	63.34	66.86	73.46
	V3off	76.10	47.36	58.06	64.37	67.16	74.49
Data from leaf-on season	V1on	66.72	47.21	54.69	58.94	63.20	59.09
	V2on	72.14	59.68	68.48	65.98	72.29	78.59
	V3on	73.02	54.84	70.09	69.94	77.27	78.89
Combined data from both seasons	V1both	76.39	65.98	63.05	65.69	69.79	72.87
	V2both	80.06	66.13	78.74	75.07	83.58	84.46
	V3both	78.59	61.88	79.03	72.29	83.14	82.99

Note: V1, spectra bands, V2, V1 plus texture, vegetation indices, segmented shapes indices, and topographic variables, V3, V2 plus RCH (relative canopy height) features, MLC, maximum likelihood classifier, ANN, artificial neural networks, kNN, k-nearest neighbor, DT, decision tree, RF, random forest, SVM, support vector machine.

Under the condition of leaf-off season based on different data sources (V1off, V2off, and V3off), the best classification results are from the MLC based on V2off or V3off, and machine learning algorithms cannot improve overall classification accuracies. When spectral bands alone were used, the MLC provided the best classification accuracy of 68.6%, 10.7% to 27% higher accuracy than machine learning approaches. Use of V2off considerably improved classification accuracies from 41.4% to 68.6% to 45.5% to 76.1%. For the leaf-on season, the best classification results were from SVM based on V2on or V3on with overall accuracies of 78.6% and 78.9%, respectively. When only spectral bands were used, MLC provided the best accuracy of 66.7% when comparing machine learning algorithms with overall accuracies of 47.2% to 63.2%. When V2on was used, SVM provided the best accuracy with 78.6%, which was 6.4% higher than MLC, and 5.4% to 19.5% higher than using V1on for all algorithms. Compared to V2on, use of V3on slightly improved overall accuracy by 0.3% to 5.0% for all algorithms except ANN.

The classification results in Table 5 indicate that MLC has better accuracy in the leaf-off season than in the leaf-on season for different data sources, but reverses for machine learning algorithms except kNN based on V2off. The combination of both leaf-off and leaf-on seasons provided better accuracy for all classification results than single seasons, which implies the important role of using multi-seasonal information to improve land-cover classification accuracy. In particular, RF and SVM based on V2both provided the best accuracy with 83.6% to 84.5%. For example, the best results using SVM based on the combination of both seasonal data and V2both was 8.4% higher than the best result using MLC based on V2off, and 5.6% higher than the best results using SVM and V3on.

In order to better understand the classification confusions between land cover types, an error matrix is provided in Table 6 as an example of the classification results using SVM based on three data

scenarios—V2off, V2on, and V2both. The classification confusion of different land covers between leaf-off and leaf-on seasons varied. For example, larch is a deciduous needle tree species and is not confused with evergreen needle tree species such as CP and MSP using V2off, but they are seriously confused using V2on. AAE is two deciduous broadleaf tree species, which was mainly distributed along roads and around villages and they are confused with croplands and ISA using V2off, but they can be separated using V2on. Grass can be confused with different land covers such as larch, birch, AAE, OBL, FL, BL, and ISA using V2off, but such confusion can be considerably reduced using V2on. Table 5 indicates that the data from different seasons have various performance in land cover classification. Larch, CP, MSP, and RP have better classification accuracy using V2off than using V2on, but AAE, OBL, shrub, and ISA are inverse. Table 6 further indicates that use of V2both can improve classification accuracies for some land cover types such as larch, birch, and AAE. As shown in Table 5, the overall classification using SVM based on V2both has the best accuracy of 84.5%, comparing with the overall accuracy of 73.5% using V2off and 78.6% using V2on, which implies the value of combining different seasonal variables in improving land cover classification.

Table 6. The error matrix of classification results based on V2off, V2on, and V2both using the support vector machine.

Accuracy Assessment Results Based on V2off Data Using Support Vector Machine															
Type	Larch	CP	MSP	RP	Birch	AAE	OBL	Shrub	Grass	FL	BL	Water	ISA	UA	PA
Larch	51	0	0	0	6	0	3	5	3	1	2	0	0	71.8	87.9
CP	0	80	3	0	0	1	0	0	1	1	1	0	0	92.0	84.2
MSP	0	4	28	0	0	0	0	0	0	0	0	0	0	87.5	90.3
RP	0	8	0	30	0	0	0	0	0	0	0	0	0	79.0	100
Birch	0	3	0	0	50	0	8	1	5	0	1	0	0	73.5	84.7
AAE	1	0	0	0	0	36	0	1	4	6	1	0	1	72.0	83.7
OBL	2	0	0	0	2	0	39	4	7	0	1	0	0	70.9	75.0
Shrub	1	0	0	0	0	0	1	34	2	1	3	0	0	81.0	64.2
Grass	3	0	0	0	1	0	1	4	32	5	5	0	2	60.4	47.1
FL	0	0	0	0	0	3	0	2	6	56	5	1	2	74.7	65.9
BL	0	0	0	0	0	0	0	2	4	0	21	0	0	77.8	44.7
Water	0	0	0	0	0	0	0	0	0	0	2	18	0	90.0	60.0
ISA	0	0	0	0	0	3	0	0	4	15	5	11	26	40.6	83.9
Accuracy assessment results based on V2on data using support vector machine															
Larch	47	8	2	0	7	1	0	6	2	0	0	0	0	64.4	81.0
CP	2	67	3	0	4	0	0	0	0	0	0	0	0	88.2	70.5
MSP	5	12	26	0	0	0	0	0	0	0	0	0	0	60.5	83.9
RP	0	1	0	30	0	0	0	0	0	0	0	0	0	96.8	100
Birch	2	2	0	0	47	0	5	2	2	0	0	0	0	78.3	79.7
AAE	0	4	0	0	0	39	0	0	1	3	0	3	0	78.0	90.7
OBL	0	0	0	0	1	0	47	0	0	0	0	0	0	97.9	90.4
Shrub	1	1	0	0	0	0	0	39	3	1	0	0	0	86.7	73.6
Grass	1	0	0	0	0	2	0	5	52	10	1	0	0	73.2	76.5
FL	0	0	0	0	0	0	0	1	2	56	7	0	0	84.9	65.9
BL	0	0	0	0	0	1	0	0	6	6	36	0	0	73.5	76.6
Water	0	0	0	0	0	0	0	0	0	1	0	19	0	95.0	63.3
ISA	0	0	0	0	0	0	0	0	0	8	3	8	31	62.0	100
Accuracy assessment results based on V2both data using the support vector machine															
Larch	55	0	0	0	11	0	0	2	1	0	0	0	0	79.7	94.8
CP	0	74	2	0	0	0	0	0	0	0	0	0	0	97.4	77.9
MSP	0	8	29	0	0	0	0	0	0	0	0	0	0	78.4	93.6
RP	0	12	0	30	0	0	0	0	0	0	0	0	0	71.4	100
Birch	0	0	0	0	46	0	3	2	0	0	0	0	0	90.2	78.0
AAE	0	0	0	0	0	39	0	0	1	1	0	0	0	95.1	90.7
OBL	0	0	0	0	1	0	49	0	1	0	0	0	0	96.1	94.2
Shrub	1	1	0	0	1	0	0	38	2	1	1	0	0	84.4	71.7
Grass	2	0	0	0	0	1	0	5	52	6	0	1	0	77.6	76.5
FL	0	0	0	0	0	3	0	1	8	71	8	1	2	75.5	83.5
BL	0	0	0	0	0	0	0	5	3	6	37	1	0	71.2	78.7
Water	0	0	0	0	0	0	0	0	0	0	0	27	0	100.0	90.0
ISA	0	0	0	0	0	0	0	0	0	0	1	0	29	96.7	93.6

Note: CP, Chinese pine, MSP, Mongolia scotch pine, RP, red pine, AAE, aspen and elm, OBL, other broadleaf tree species, FL, farmland, BL, bare land, and ISA, impervious surface area.

Figure 5 illustrates the land-cover classification result highlighting forest types using SVM based on spectral bands, vegetation indices, textures, and topographic factors from the combination of both seasons (i.e., V2both). Larch and CP are needle-leaf tree species that accounted for 26.8% and 13.5%, respectively, of the entire study area (Table 7), especially near roads and villages where people can access easily, while MSP and RP cover very little area, accounting for only 0.8%. Most broadleaf tree species are natural forests with birch and other broadleaf forests accounting for 15.1% and 7%, respectively. These tree species are mainly distributed in the southwest and southeast of the study area where elevation is relatively higher than where needle-leaf tree species occur. AAE is distributed mainly in the flat areas near villages and roads.

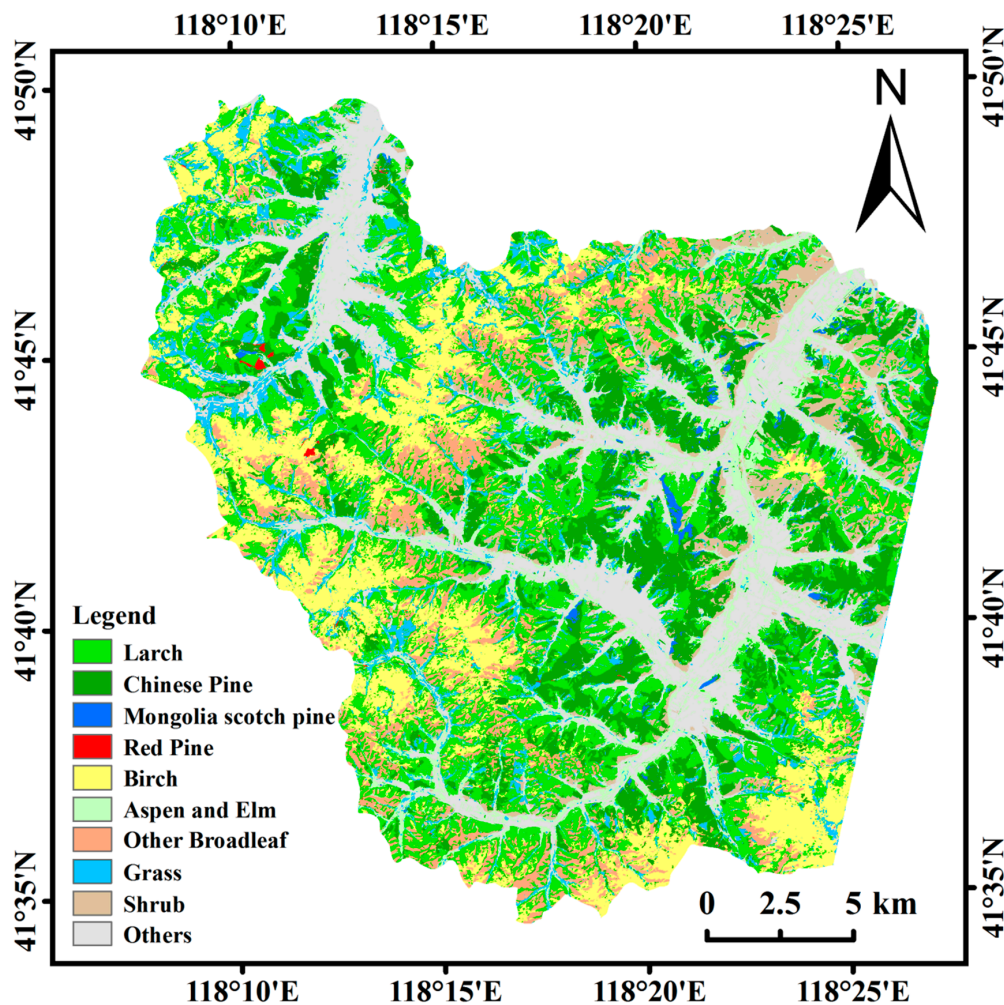


Figure 5. Land-cover classification result using a support vector machine based on spectral response, textures, and topographic factors from the combination of leaf-off and leaf-on seasons.

Table 7. Area of all land-cover types in this study.

Land-Cover Type	Area (km ²)	%
Larch	133.89	26.78
Birch	75.50	15.10
Chinese pine	67.22	13.45
Aspen and elm	36.08	7.22
Other broadleaf tree species	35.04	7.01
Mongolia scotch pine	3.60	0.72
Red pine	0.55	0.11
Grass	33.21	6.64
Shrub	32.78	6.56
Farmland	58.30	11.66
Impervious surface area	12.74	2.55
Bare land	10.48	2.10
Water	0.48	0.10

3.1.2. Classification Results Based on Overall Forest Classes

Table 5 provided the summary of land-cover classification accuracies, and Table 8 provides the forest-cover classification accuracy based on the same data scenarios. Most conclusions are similar, but there are some exceptions. For example, addition of RCH features in the leaf-on season can provide better classification accuracy when RF or kNN is used. RF based on V3on improved by 9.5% and kNN by 4.8% compared to using V2on while adding RCH features in the leaf-off season yields no or very little improvement, except with ANN. Table 8 also indicates that combining leaf-off and leaf-on images considerably improved classification accuracy compared to single-season images for all data scenarios. The classification procedure based on V2 (off, on, or both) using MLC or SVM is recommended for either a single season or combined seasons, and the overall forest classification accuracy can be 82.3% to 89.2%.

Table 8. The summary of overall average accuracies of all forest types among six classification algorithms based on different data sources.

Data Scenarios		Overall Forest Classification Accuracies (%) Based on Six Algorithms					
		MLC	ANN	kNN	DT	RF	SVM
Data from leaf-off season	V1off	80.96	34.79	62.26	61.06	69.65	67.41
	V2off	84.09	44.77	81.48	73.67	71.47	82.33
	V3off	82.85	55.90	65.99	73.92	72.91	81.78
Data from leaf-on season	V1on	76.43	54.44	63.02	67.81	70.13	59.05
	V2on	82.42	62.32	71.90	74.88	73.51	82.87
	V3on	83.61	54.98	76.66	75.48	83.01	84.76
Combined data from both seasons	V1both	88.20	71.19	71.44	71.75	76.08	76.07
	V2both	89.22	72.41	85.02	82.12	88.12	88.39
	V3both	89.41	68.14	85.85	82.15	88.78	88.16

Note: V1, spectra bands, V2, V1 plus texture, vegetation indices, segmented shapes indices, and topographic variables, V3, V2 plus RCH features, MLC, maximum likelihood classifier, ANN, artificial neural networks, kNN, k-nearest neighbor, DT, decision tree, RF, random forest, SVM, support vector machine.

3.1.3. Synthetic Analysis of Classification Results

By re-organizing Tables 5 and 8 into Table 9, the accuracy assessment results indicate that combination of the images at leaf-on and leaf-off seasons improved land cover classification by 2.5% to 15.0% and forest classification accuracy by 4.0% to 11.8%. In particular, if only spectral bands were used, use of bi-seasonal images improved land cover classification accuracy by 7.8% to 15.0% and forest classification accuracy by 6.0% to 11.8%. Comparing V2 data sets with V1, the land cover classification accuracy was improved by 3.7% to 15.5% and forest classification accuracy by 1.0% to 12.7%. In particular, use of machine learning algorithm based on V2, the land cover classification accuracy can be improved by over 15.4% and forest classification accuracy by 12.7% for either leaf-off or leaf-on images. While comparing V3 with V2, the incorporation of RCH features has no or limited effects on improving overall land cover or forest classification accuracy. However, when leaf-on images

were used, the addition of RCH features can slightly improve forest classification accuracy by 1.2% to 1.9%. Table 9 also indicates that, during the leaf-off season, the machine learning algorithm cannot improve land cover or forest classification accuracy comparing to MLC no matter which data sets, V1, V2, or V3, were used. The same situation included using only spectral bands from leaf-on images. However, machine learning improved land cover or forest classification when V2 or V3 data sets were used, especially the land cover classification accuracy, which can be improved by 6.5% for V2 and by 5.9% for V3. The results in Table 9 showed that, when only spectral bands were used, MLC is recommended. However, when multiple sources of data were used, machine learning, especially SVM, is recommended. Overall, SVM based on multiple source data with the combination of leaf-on and leaf-off seasons is recommended, with land cover classification accuracy of 84.5%.

Table 9. A summary of accuracy assessment results based on different data sources and classification methods, according to overall land cover and forest class by re-organizing Tables 5 and 8.

Category	Dataset	Approach	Accuracy Based on Seasonal Data			Difference Between	
			Different Seasons		Comb. of Both Seasons	Comb. & Leaf-Off	Comb. & Leaf-On
			leaf-off	leaf-on			
All land cover types	V1	Maximum likelihood	68.62	66.72	76.39	7.77	9.67
		Machine learning	57.92	63.20	72.87	14.95	9.67
	V2	Maximum likelihood	76.10	72.14	80.06	3.96	7.92
		Machine learning	73.46	78.59	84.46	11.00	5.87
	V3	Maximum likelihood	76.10	73.02	78.59	2.49	5.57
		Machine learning	74.49	78.89	83.14	8.65	4.25
All forest types	V1	Maximum likelihood	80.96	76.43	88.20	7.24	11.77
		Machine learning	69.65	70.13	76.08	6.43	5.95
	V2	Maximum likelihood	84.09	82.42	89.22	5.13	6.80
		Machine learning	82.33	82.87	88.39	6.06	5.52
	V3	Maximum likelihood	82.85	83.61	89.41	6.56	5.80
		Machine learning	81.78	84.76	88.78	7.00	4.02
All land cover types	v2&v1	Maximum likelihood	7.48	5.42	3.67		
		Machine learning	15.54	15.39	11.59		
	v3&v2	Maximum likelihood	0.00	0.88	-1.47		
		Machine learning	1.03	0.30	-1.32		
All forest types	v2&v1	Maximum likelihood	3.13	5.99	1.02		
		Machine learning	12.68	12.74	12.31		
	v3&v2	Maximum likelihood	-1.24	1.19	0.19		
		Machine learning	-0.55	1.89	0.39		

Note: The bold numbers in this table indicate the highest classification accuracies corresponding to different scenarios.

3.2. Comparative Analysis of Classification Results Based on Tree Species

Larch and birch are deciduous tree species and have relatively lower classification accuracies than other tree species no matter what data sources are used (Table 10). Generally, all tree species, except OBL, have relatively better classification accuracies using leaf-off seasonal data than using leaf-on seasonal data, and the combination of both considerably improves classification accuracy for each tree species. All tree species except larch have better classification accuracies using spectral response, textures, and topographic factors (V2) than using only spectral signatures (V1). However, the addition of RCH features into V2 data may or may not improve classification accuracy, depending on specific tree species. For example, use of RCH features is especially helpful for improving mapping accuracies of Chinese pine and birch in leaf-off season. While in leaf-on season, incorporation of RCH features into remotely sensed data can improve classification accuracies of all forest types except Chinese pine. The results in Table 10 implied the important value using the RCH features in forest classification, but also indicated that no one data source and no one classification algorithm can provide the best classification accuracy for all tree species. This situation required the need to develop a comprehensive classification procedure for tree species classification.

Table 10. Summary of the best classification accuracy for each tree species based on different classification algorithms and different data sources.

Tree Species Type	Data from Leaf-Off Season			Data from Leaf-On Season			Combined Both Seasons		
	Data	Classifier	TSMA (%)	Data	Classifier	TSMA (%)	Data	Classifier	TSMA (%)
Larch	V1	MLC	80.1	V1	MLC	77.2	V1	MLC	83.6
	V2	SVM/kNN	79.9/79.3	V2	SVM/MLC	72.7/71.8	V2	SVM	87.3
	V3	SVM	77.7	V3	RF/SVM	73.6/73.0	V3	SVM/RF	86.7/86.3
Chinese pine	V1	kNN	89.2	V1	DT/MLC	79.2/78.8	V1	MLC	92.5
	V2	MLC/SVM	89.2/88.1	V2	MLC	83.6	V2	RF/MLC	91.6/91.4
	V3	MLC	91.4	V3	MLC	82.9	V3	RF/MLC	92.2/91.4
Mongolia scotch pine	V1	MLC	87.9	V1	kNN/MLC	80.1/79.6	V1	MLC	96.8
	V2	SVM/MLC	88.9/88.6	V2	MLC	81.1	V2	MLC/kNN	93.6/92.5
	V3	MLC	90.1	V3	RF	91.2	V3	kNN/MLC	93.8/93.6
Red pine	V1	MLC/kNN	96.7/96.7	V1	RF/kNN	98.3/98.3	V1	MLC/RF	96.7/96.7
	V2	MLC	98.3	V2	SVM/MLC	98.4/98.3	V2	DT/MLC	98.4/96.7
	V3	MLC	98.3	V3	SVM/MLC	98.4/98.3	V3	DT	100
Birch	V1	MLC	68.2	V1	MLC	57.9	V1	MLC	78.5
	V2	SVM	79.1	V2	MLC/SVM	79.7/79.0	V2	SVM/MLC	84.1/82.5
	V3	SVM	84.5	V3	MLC/SVM	81.7/80.8	V3	SVM/MLC	84.1/82.5
Aspen and elm	V1	MLC	65.3	V1	MLC	58.5	V1	MLC	74.4
	V2	kNN/MLC	83.0/80.1	V2	SVM	84.4	V2	SVM	92.9
	V3	SVM	80.8	V3	SVM	85	V3	SVM	94.3
Other broadleaf trees	V1	MLC	82.1	V1	RF/ANN	90.4/90.1	V1	MLC/RF	95.1/93.3
	V2	kNN	91.1	V2	SVM	94.2	V2	MLC/SVM	95.2/95.2
	V3	MLC	74.1	V3	DT/RF	93.5/92.3	V3	MLC/RF	96.2/96.2

Note: V1, spectra bands, V2, V1 plus texture, vegetation indices, segmented shapes indices, and topographic variables, V3, V2 plus RCH features, MLC, maximum likelihood classifier, SVM, support vector machine, kNN, k-nearest neighbor, TSMA, tree species mapping accuracy, RF, random forest, DT, decision tree, and ANN, artificial neural networks. The bold numbers in this table indicate the highest classification accuracies corresponding to different scenarios.

4. Discussion

4.1. Use of Seasonal Information to Improve Forest Classification Accuracy

Use of seasonal vegetation information or phenological features has long been regarded as valuable for vegetation classification [19,27], in particular when medium spatial resolution images such as Landsat were used for such studies as forest disturbance. For a single-season image, the similar spectral signatures among green vegetation types in a leaf-on image or among the deciduous tree species in the leaf-off season often resulted in misclassification [15,98]. Different seasonal images have their own advantages and disadvantages. For example, in the growing season, larch (deciduous) and Chinese pine (evergreen), which are both needle-leaf tree species, can be misclassified, but, during the winter season, they can be separated easily because of their different spectral signatures. In contrast, larch and birch, which are both deciduous tree species, can be misclassified in the winter but easily separated in the growing season because larch is needle-leaf and birch is broadleaf, and they have different spectral signatures. Therefore, the combination of both seasonal images can considerably improve classification accuracy, as shown in the classification accuracy results in this research (Table 9) that use of both leaf-on and leaf-off images can improve overall land cover accuracy by 15% and forest classification by 11.8%. Similar conclusions were also obtained in previous studies [19,26,99]. With high spatial resolution images, such as QuickBird, Worldview, Pleiades, and SPOT 6, multi-seasonal high spatial resolution images have been used for vegetation classification [21]. However, such studies mainly focused on relatively small study areas at present, considering the cost of purchasing images and the large volume of data [72]. As easy availability of high spatial resolution satellite images with different kinds of sensors and use of high-speed computers, application of using multiple-seasonal high spatial resolution satellite images will be an important research topic in the near future for detailed classification of land covers or forest types.

4.2. The Roles of Spatial and Topographic Features

The spectral signature is often the most important feature in land-cover classification, especially for medium and coarse spatial resolution images [27,80]. In high-resolution images, spatial information

becomes another important feature in improving land-cover classification [19,21,31,100]. This research also confirmed the important role of spatial features, especially for the separation between needle-leaf and broadleaf tree species because of their different stand structures and canopy sizes. As shown in Table 9, comparing to only spectral signatures, use of multiple source data can improve land cover classification accuracy by 15.5% and forest accuracy by 12.7%, which implies the necessity of effective incorporation of different data sources in a classification procedure [27]. Texture is often extracted using GLCM based on a spectral image and a fixed window size such as 5×5 . However, the performance of using textures depends on specific land-cover types and patch sizes. Thus, they may be effective for some land-cover types but not good for others [28]. This research used the segmented polygons to calculate textures to avoid the problem using a fixed window size. However, development of a high-quality segment image becomes a critical step, which is often time-consuming and requires optimization of the parameters used in the eCognition software.

Topographic variables such as slope and elevation are useful features in improving land-cover classification [27]. For example, birch and aspen are respectively deciduous and broadleaf tree species that may be misclassified in any season, but their spatial distribution is different, since, in China, aspen is mainly planted in villages and along roads that are flat and have good water sources, whereas birch forms natural forests distributed in sloped regions. Thus, use of slope and/or elevation can separate them. In addition to the use of extra bands, topographic factors can also be used during pre-classification or post-classification modification [27]. In this case, expert knowledge about the relationships between tree species distribution and topographic factors becomes critical [27]. However, caution should be taken when topographic factors are used for land-cover or forest classification in a large area because precipitation and temperature, as well as different human activities, can affect the relationships between forest distribution and topographic factors.

The difference of stand structures between plantations and natural forests is valuable for forest or tree species classification. For example, plantations often consist of single tree species with the same age and similar canopy size and shape, while natural forests are composed of different tree species of various canopy heights, crown sizes, and ages. Thus, textures representing stand structures can improve forest classification, which is shown in previous research [28] and confirmed in this research. Incorporation of spatial features can considerably improve forest classification. The difference between spatial distribution and patterns among plantations and natural forests can also be used to improve classification performance. For example, plantations are often distributed along roads and near villages where people can easily access them, while natural forests are not. Thus, expert knowledge can be developed to support forest classification [25]. On the other hand, the spectral signatures among deciduous tree species, croplands with residuals, and even bare soils in the winter season can be similar, which result in misclassification. However, their shapes and patch sizes can be considerably different, and use of shape indices from the segmentation procedure can reduce this misclassification. This research implies that use of multiple-source information, including spectral response, textures, shape, and topographic factors, is valuable in improving land-cover or forest classification accuracy. More research is needed to effectively incorporate different data sources in this improvement. Another important research topic in the near future can be the examination of quantitative contributions of different kinds of data sources in improving land cover or forest classification.

4.3. The Role of Canopy Height Features

Canopy height could be a very useful feature in the separation of tree species, especially when very high spatial resolution images are used. Different tree species may have very different heights, crown sizes, and shapes. Therefore, different forest types may have varied stand structures, such as high or low density, due to the composition of these attributes. Previous research has indicated that incorporation of canopy height features can improve tree species classification [36,37], and the research results in Table 10 also confirmed the value using canopy height features in improving tree species such

as birch and MSP. Another important use of canopy height features may be the separation of different age groups such as young, middle, and mature groups that are often required in forest inventory but has not received much attention in remote sensing applications. The difference in forest stand structures caused by tree crown sizes and shapes may be very useful for distinguishing different forest types, especially plantations (between needle-leaf plantations and broadleaf plantations) and natural forest (single tree and mixed tree species). More research is needed to explore how to effectively incorporate canopy height features to improve forest classification.

Accurate extraction of canopy height is usually accomplished by using lidar data. However, for most study areas, lidar data are not available because they often come from an aerial platform. Satellite stereo images, which are now readily available, provide a new opportunity to extract canopy height images. The critical goal is to improve accuracy in extracting DSM data from satellite stereo imagery. Lack of high-quality DEM data prevent the determination of true canopy height from leaf-on and leaf-off stereo images because the impacts of evergreen tree species result in overestimation of DEM data and inconsistent accuracy between the evergreen and deciduous forest lands. Additionally, canopy height cannot directly be used for separation of tree species. The most important step is to identify one or more suitable attributes to represent the differences in forest stand structures between different kinds of tree species. RCH is not true canopy or tree height because of deciduous and evergreen forest types, but use of this RCH features is valuable for separating larch and MCP during the growing season, and the deciduous forest and non-vegetation types (fields) during the winter season. The canopy height features have not been extensively applied in forest or tree species classification yet. More research is needed to identify suitable attributes representing the differences in canopy structures among different forest types or age groups.

4.4. Selection of a Suitable Classification Algorithm

Although many classification algorithms, from a minimum distance, MLC, and cluster analysis to machine learning such as ANN and SVM, have been explored for land-cover classification, it is unclear which approach can provide the best performance. Success depends on many factors such as the characteristics of the study area under investigation, the classification system, remotely sensed data, use of ancillary data, and the skills of the analyst [27]. Many previous studies have conducted comparative analyses of different classification algorithms [63,64,80,101], but no consistent conclusions were obtained. Our research compared six classifiers based on different data sources in two seasons, and the performances varied depending on the seasons and data scenarios. However, some common conclusions were obtained. For example, when only spectral signatures were used for classification, MLC provided better classification results than machine learning algorithms, which is similar to an earlier conclusion in tropical forest classification [64,80]. However, when multi-source data were used, RF and SVM provided better classification results than MLC. As shown in Table 9, the machine learning algorithm based on multiple source data at the leaf-on season can improve land cover classification accuracy of 6.5% compared to use of MLC. This research also indicates that, no matter which classification approaches are selected, researchers should consider the characteristics of data sources and classification system (land cover, forest type, or tree species). This research result confirms that different classification algorithms have their own merits and shortcomings, which result in better classification accuracy for some land cover types than others. This is a similar conclusion produced in previous studies [63,64]. Therefore, a decision-level fusion approach can be used to combine the classification results from different classification algorithms or using different data sets to produce an improved classification result [27].

The object-based approaches have become attractive in recent years due to extensive use of high spatial resolution images [102–104]. Previous studies have proven that the object-based approaches can provide better classification accuracy than pixel-based approaches, especially when high spatial resolution images are used [21,36,104–106]. One step in the object-based approach is to optimize the parameters to produce the best segmentation image. However, it is often a challenge to identify

the optimal parameters due to the subjective criteria and the complexity of land-cover composition and variety of patch sizes. To date, there are no standard approaches to determine the parameters for a given study. It depends on the analyst and characteristics of the study area. More research should be paid to examining how spatial resolution, different kinds of data (e.g., spectral bands, textures, ancillary data), and different kinds of landscapes (e.g., urban, forest, wetland) influence the determination of optimal parameters. We need to establish general guidelines to quickly optimize parameters to produce quality segmentation results.

4.5. The Need to Develop a Comprehensive Procedure for Forest Classification

Many previous studies explored approaches to extract a single tree species such as rubber, eucalyptus, Chinese fir, pine, or hickory using medium or high spatial resolution images [11,15,25,107]. However, extraction of multiple tree species becomes much complicated due to the complex composition of different tree species in a landscape and limitation of remotely sensed data. This research (Table 10) indicated that spectral signatures were still the most important feature in tree species classification, but combinations of different seasonal images can improve classification accuracy. Incorporation of different source data such as textures, topographic factors, and canopy height further improves classification. However, because there are many potential variables that can be used in forest classification, the critical goal is to identify the variables that can effectively distinguish forest types. Therefore, more research should be focused on the exploration of the relationships of remote sensing variables and forest types. Since RF provides an effective way to identify the important variables for forest classification, research can focus on the selected variables and forest types to better understand the mechanisms of remote sensing variables in separating different forest types.

This research indicated that success of a classification depends on the selection of suitable variables from different data sources and seasons and selection of a suitable classification algorithm. It is necessary to develop a comprehensive classification procedure that can effectively integrate different data sources and algorithms for specific tree species. Currently, there is no such procedure for tree species classification. The critical step is to determine which variable or variables and which algorithm should be selected for mapping different tree species. A promising approach may be to use the deep learning approach that can use multiple data sources for detailed land cover classification [43,44]. Other potential solutions could be using hierarchical-based classification or expert-based classification [19,25].

5. Conclusions

Detailed tree species classification using high spatial resolution imagery is a challenging task due to the limitation of remotely sensed data, complexity of tree species spatial patterns and compositions, and lack of suitable approaches. We explored using ZY-3 multi-spectral and stereo images from leaf-on and leaf-off seasons to map land cover, forest, and tree species distributions using six classification algorithms (ANN, kNN, MLC, SVM, DT, RF) under different data scenarios, including spectral responses, textures, canopy height features, and topographic factors. The major conclusions can be summarized as follows:

- (1) If only spectral bands are used, MLC provides better land-cover or forest classification results than machine learning algorithms. MLC based on the combination of leaf-on and leaf-off spectral data can produce overall land cover classification of 76.4% and overall forest classification of 88.2% compared with the best results from machine learning algorithm with 72.9% for overall land covers and 76.1% for forest classes.
- (2) A leaf-off season image provides better classification results than a leaf-on image, and the combination of leaf-on and leaf-off images considerably improves the classification accuracy. The combination of leaf-on and leaf-off images can improve land cover classification accuracy by 15% and forest classification by 11.8%, which implies the necessity of using bi-temporal images for land cover or forest classification in the temperate climate zones.

- (3) Comparing only spectral bands, incorporation of multi-source data such as spectral responses, textures, and topographic factors can considerably improve classification, especially when machine learning algorithms such as RF and SVM are used. The overall land cover classification accuracy can be improved by 15.5% and forest by 12.7% using multiple source data compared to using spectral data alone, which implies the necessity of using multiple source data in land cover or forest classification in mountainous regions.
- (4) The addition of canopy height features may or may not improve forest classification, but can improve it for some tree species such as birch in leaf-off season and MSP in the leaf-on season. As accurate canopy height image can be extracted from lidar or from the combination of lidar and satellite stereo images, effective incorporation of canopy height features that can represent the difference of forest stand structures among different forest types into remotely sensed data will be a new research topic in improving forest classification.
- (5) Considering overall land-cover classification, RF and SVM provided the best classification accuracy of about 84%. Considering the overall forest classification, MLC provided the best accuracy of more than 89%, which is followed by RF and SVM with overall accuracy of more than 88%. Considering single tree species including larch, birch, and AAE had relatively lower classification accuracies than CP, MSP, RP, and OBL, and no single classification algorithm or data source provided the best accuracy for all tree species. This research implies the requirement to develop a comprehensive classification procedure that can employ specific approaches corresponding to different tree species. As high-performance computers and large volumes of different source data become available, deep learning approaches may be the new research directions for accurately mapping tree species distribution.

Author Contributions: Conceptualization, D.L. and E.C. methodology, D.L., Z.X., Y.C., G.L., and E.C. software, Z.X. validation, Z.X., Y.C., and G.L. formal analysis, Z.X., Y.C., and G.L. investigation, Z.X., Y.C., G.L., and D.L. resources, Z.X. data curation, Z.X. writing original draft, D.L., Z.X., and Y.C. review and editing, D.L. and G.L. visualization, D.L. supervision, D.L. project administration, D.L. and E.C. funding acquisition, D.L. and E.C.

Funding: This research is financially supported by the National Key R&D Program of China project “Research of Key Technologies for Monitoring Forest Plantation Resources” (2017YFD0600900).

Acknowledgments: The authors would like to thank Lei Zhao, Longwei Li, Xiandie Jiang, Xiaozhi Yu, and Yahui Wang for their help in the fieldwork.

Conflicts of Interest: The authors declare no conflict of interest.

References

1. Brockerhoff, E.G.; Jactel, H.; Parrotta, J.A.; Quine, C.P.; Sayer, J. Plantation forests and biodiversity: Oxymoron or opportunity? *Biodivers. Conserv.* **2008**, *17*, 925–951. [[CrossRef](#)]
2. Shang, X.; Chisholm, L.A. Classification of Australian native forest species using hyperspectral remote sensing and machine-learning classification algorithms. *IEEE J.-STARS* **2014**, *7*, 2481–2489. [[CrossRef](#)]
3. Zhao, P.; Lu, D.; Wang, G.; Wu, C.; Huang, Y. Examining spectral reflectance saturation in Landsat imagery and corresponding solutions to improve forest aboveground biomass estimation. *Remote Sens.* **2016**, *8*. [[CrossRef](#)]
4. Feng, Y.; Lu, D.; Chen, Q.; Keller, M.; Moran, E.; Dos-Santos, M.N.; Bolfe, E.L.; Batistella, M. Examining effective use of data sources and modeling algorithms for improving biomass estimation in a moist tropical forest of the Brazilian Amazon. *Int. J. Digit. Earth* **2017**, *10*, 996–1016. [[CrossRef](#)]
5. Tao, B.; Tian, H.; Chen, G.; Ren, W.; Lu, C.; Alley, K.D.; Xu, X.; Liu, M.; Pan, S.; Virji, H. Terrestrial carbon balance in tropical Asia: Contribution from cropland expansion and land management. *Glob. Planet. Chang.* **2013**, *100*, 85–98. [[CrossRef](#)]
6. Ray, D.; Bathgate, S.; Moseley, D.; Taylor, P.; Nicoll, B.; Pizzirani, S.; Gardiner, B. Comparing the provision of ecosystem services in plantation forests under alternative climate change adaptation management options in Wales. *Reg. Environ. Chang.* **2015**, *15*, 1501–1513. [[CrossRef](#)]

7. D'Amato, D.; Rekola, M.; Wan, M.; Cai, D.; Toppinen, A. Effects of industrial plantations on ecosystem services and livelihoods: Perspectives of rural communities in China. *Land Use Policy* **2017**, *63*, 266–278. [[CrossRef](#)]
8. Xiao, X.; Boles, S.; Liu, J.; Zhuang, D.; Liu, M. Characterization of forest types in Northeastern China, using multi-temporal SPOT-4 VEGETATION sensor data. *Remote Sens. Environ.* **2002**, *82*, 335–348. [[CrossRef](#)]
9. Lin, C. China Forest Bureau announced the results of the fifth national forest resource inventory. *Sci. Silv. Sin.* **2000**, *36*, 105.
10. China Forest Bureau. *China Forest Resource Report (2008–2013)*; China Forestry Publishing House: Beijing, China, 2014; ISBN 9787503874246.
11. Alatorre, L.C.; Sánchezandrés, R.; Cirujano, S.; Beguería, S.; Sánchezcarrillo, S. Identification of mangrove areas by remote sensing: The ROC curve technique applied to the northwestern Mexico coastal zone using Landsat imagery. *Remote Sens.* **2011**, *3*, 1568–1583. [[CrossRef](#)]
12. Kempeneers, P.; Sedano, F.; Seebach, L.; Strobl, P.; San-Miguel-Ayanz, J. Data fusion of different spatial resolution remote sensing images applied to forest-type mapping. *IEEE Trans. Geosci. Remote* **2011**, *49*, 4977–4986. [[CrossRef](#)]
13. Zhang, Y.; Lu, D.; Yang, B.; Sun, C.; Sun, M. Coastal wetland vegetation classification with a Landsat Thematic Mapper image. *Int. J. Remote Sens.* **2011**, *32*, 545–561. [[CrossRef](#)]
14. Han, X.; Chen, X.; Feng, L. Four decades of winter wetland changes in Poyang Lake based on Landsat observations between 1973 and 2013. *Remote Sens. Environ.* **2015**, *156*, 426–437. [[CrossRef](#)]
15. Dong, J.; Xiao, X.; Chen, B.; Torbick, N.; Jin, C.; Zhang, G.; Biradar, C. Mapping deciduous rubber plantations through integration of PALSAR and multi-temporal Landsat imagery. *Remote Sens. Environ.* **2013**, *134*, 392–402. [[CrossRef](#)]
16. Qiao, H.; Wu, M.; Shakir, M.; Wang, L.; Kang, J.; Zheng, N. Classification of small-scale eucalyptus plantations based on NDVI time series obtained from multiple high-resolution datasets. *Remote Sens.* **2016**, *8*, 117. [[CrossRef](#)]
17. Gomez, C.; Mangeas, M.; Petit, M.; Corbane, C.; Hamon, P. Use of high-resolution satellite imagery in an integrated model to predict the distribution of shade coffee tree hybrid zones. *Remote Sens. Environ.* **2010**, *114*, 2731–2744. [[CrossRef](#)]
18. Han, N.; Wang, K.; Yu, L.; Zhang, X. Integration of texture and landscape features into object-based classification for delineating *Torreya* using IKONOS imagery. *Int. J. Remote Sens.* **2012**, *33*, 2003–2033. [[CrossRef](#)]
19. Li, N.; Lu, D.; Wu, M.; Zhang, Y.; Lu, L. Coastal wetland classification with multiseasonal high-spatial resolution satellite imagery. *Int. J. Remote Sens.* **2018**. [[CrossRef](#)]
20. Xi, Z.; Lu, D.; Liu, L.; Ge, H. Detection of drought-induced hickory disturbances in western Lin'An county, China, using multitemporal Landsat imagery. *Remote Sens.* **2016**, *8*. [[CrossRef](#)]
21. Lu, D.; Hetrick, S.; Moran, E. Land cover classification in a complex urban-rural Landscape with QuickBird imagery. *Photogramm. Eng. Remote Sens.* **2010**, *76*, 1159–1168. [[CrossRef](#)]
22. Johnson, B.; Xie, Z. Classifying a high resolution image of an urban area using super-object information. *ISPRS J. Photogramm.* **2013**, *83*, 40–49. [[CrossRef](#)]
23. Feng, Y.; Lu, D.; Moran, E.; Dutra, L.; Calvi, M.; De Oliveira, M. Examining spatial distribution and dynamic change of urban land covers in the Brazilian Amazon using multitemporal multisensor high spatial resolution satellite imagery. *Remote Sens.* **2017**, *9*, 381. [[CrossRef](#)]
24. Cho, M.A.; Malahlela, O.; Ramoelo, A. Assessing the utility WorldView-2 imagery for tree species mapping in South African subtropical humid forest and the conservation implications: Dukuduku forest patch as case study. *Int. J. Appl. Earth Obs.* **2015**, *38*, 349–357. [[CrossRef](#)]
25. Wang, Y.; Lu, D. Mapping *Torreya grandis* spatial distribution using high spatial resolution satellite imagery with the expert rules-based approach. *Remote Sens.* **2017**, *9*. [[CrossRef](#)]
26. Reis, S.; Taşdemir, K. Identification of hazelnut fields using spectral and Gabor textural features. *ISPRS J. Photogramm.* **2011**, *66*, 652–661. [[CrossRef](#)]
27. Lu, D.; Weng, Q. A survey of image classification methods and techniques for improving classification performance. *Int. J. Remote Sens.* **2007**, *28*, 823–870. [[CrossRef](#)]
28. Lu, D.; Li, G.; Moran, E.; Dutra, L.; Batistella, M. The roles of textural images in improving land-cover classification in the Brazilian Amazon. *Int. J. Remote Sens.* **2014**, *35*, 8188–8207. [[CrossRef](#)]
29. Immitzer, M.; Atzberger, C.; Koukal, T. Tree species classification with random forest using very high spatial resolution 8-band WorldView-2 satellite data. *Remote Sens.* **2012**, *4*, 2661–2693. [[CrossRef](#)]

30. Zhang, X.; Du, S. Learning selfhood scales for urban land cover mapping with very-high-resolution satellite images. *Remote Sens. Environ.* **2016**, *178*, 172–190. [[CrossRef](#)]
31. Dihkan, M.; Guneroglu, N.; Karsli, F.; Guneroglu, A. Remote sensing of tea plantations using an SVM classifier and pattern-based accuracy assessment technique. *Int. J. Remote Sens.* **2013**, *34*, 8549–8565. [[CrossRef](#)]
32. Lu, D.; Moran, E.; Batistella, M. Linear mixture model applied to Amazonian vegetation classification. *Remote Sens. Environ.* **2003**, *87*, 456–469. [[CrossRef](#)]
33. Lu, D. Integration of vegetation inventory data and Landsat TM image for vegetation classification in the western Brazilian Amazon. *For. Ecol. Manag.* **2005**, *213*, 369–383. [[CrossRef](#)]
34. Holmgren, J.; Persson, Å.; Söderman, U. Species identification of individual trees by combining high resolution LiDAR data with multi-spectral images. *Int. J. Remote Sens.* **2008**, *29*, 1537–1552. [[CrossRef](#)]
35. Eetu, P.; Juha, S.; Teemu, H.; Esa, R.; Harri, K.; Sanna, K.; Paula, L. Tree species classification from fused active hyperspectral reflectance and LIDAR measurements. *For. Ecol. Manag.* **2010**, *260*, 1843–1852. [[CrossRef](#)]
36. Ke, Y.; Quackenbush, L.J.; Im, J. Synergistic use of QuickBird multispectral imagery and LIDAR data for object-based forest species classification. *Remote Sens. Environ.* **2010**, *114*, 1141–1154. [[CrossRef](#)]
37. Dalponte, M.; Bruzzone, L.; Gianelle, D. Tree species classification in the Southern Alps based on the fusion of very high geometrical resolution multispectral/hyperspectral images and LiDAR data. *Remote Sens. Environ.* **2012**, *123*, 258–270. [[CrossRef](#)]
38. Haby, N.; Tunn, Y.; Cameron, J. Application of QuickBird and aerial imagery to detect *Pinus radiata* in remnant vegetation. *Aust. Ecol.* **2010**, *35*, 624–635. [[CrossRef](#)]
39. Ferreira, M.P.; Zortea, M.; Zanotta, D.C.; Shimabukuro, Y.E. Mapping tree species in tropical seasonal semi-deciduous forests with hyperspectral and multispectral data. *Remote Sens. Environ.* **2016**, *179*, 66–78. [[CrossRef](#)]
40. Dalponte, M.; Orka, H.O.; Gobakken, T.; Gianelle, D.; Naesset, E. Tree species classification in boreal forests with hyperspectral data. *IEEE Trans. Geosci. Remote* **2013**, *51*, 2632–2645. [[CrossRef](#)]
41. Raczko, E.; Zagajewski, B. Comparison of support vector machine, random forest and neural network classifiers for tree species classification on airborne hyperspectral APEX images. *Eur. J. Remote Sens.* **2017**, *50*, 144–154. [[CrossRef](#)]
42. Chen, Y.; Lin, Z.; Zhao, X.; Wang, G.; Gu, Y. Deep learning-based classification of hyperspectral data. *IEEE J.-STARS* **2017**, *7*, 2094–2107. [[CrossRef](#)]
43. Pan, B.; Shi, Z.; Xu, X. MugNet: Deep learning for hyperspectral image classification using limited samples. *ISPRS J. Photogramm.* **2017**. [[CrossRef](#)]
44. Zou, X.; Cheng, M.; Wang, C.; Xia, Y.; Li, J. Tree classification in complex forest point clouds based on deep learning. *IEEE Geosci. Remote* **2017**, *14*, 2360–2364. [[CrossRef](#)]
45. Feng, Z.; Xie, M.; Gao, Y. Evaluation on the woodland resource value in Wangyedian trial forest farm. *For. Invent. Plan.* **2014**, *29*, 60–65.
46. Zhang, N.; Feng, Z.; Feng, Y.; Fan, J. Research on coniferous forest volume estimation model for Wangyedian experimental forest farm. *J. Cent. South Univ. For. Technol.* **2013**, *33*, 83–87.
47. Gong, Y.; He, C.; Yan, F.; Feng, Z.; Cao, M.; Gao, Y.; Miao, J.; Zhao, J. Study on artificial neural network combined with multispectral remote sensing imagery for forest site evaluation. *Spectrosc. Spect. Anal.* **2013**, *33*, 2815–2822. [[CrossRef](#)]
48. Wu, G. Wangyedian forest farm operates. *J. Inner Mongol. For.* **1989**, *1*, 11.
49. Wu, C.; Ma, C. Struggle for sixty years, dream and flourishing industry—Record of development of Wangye Dian Experimental Forest Farm in Chifeng, the Inner Mongolia Autonomous Region. *Land Green.* **2015**, *7*, 16–19.
50. Li, X.; Chen, W.; Cheng, X. A comparison of machine learning algorithms for mapping of complex surface-mined and agricultural landscapes using ZiYuan-3 stereo satellite imagery. *Remote Sens.* **2016**, *8*, 514. [[CrossRef](#)]
51. Luo, H.; Li, L.; Zhu, H.; Kuai, X.; Zhang, Z.; Liu, Y. Land cover extraction from high resolution ZY-3 satellite imagery using ontology-based method. *ISPRS Int. J. Geo-Inf.* **2016**, *5*, 31. [[CrossRef](#)]
52. Gu, H.; Li, H.; Yan, L.; Liu, Z.; Blaschke, T.; Soergel, U. An object-based semantic classification method for high resolution remote sensing imagery using ontology. *Remote Sens.* **2017**, *9*, 329. [[CrossRef](#)]
53. Chander, G.; Markham, B.L.; Helder, D.L. Summary of current radiometric calibration coefficients for Landsat MSS, TM, ETM+, and EO-1 ALI sensors. *Remote Sens. Environ.* **2009**, *113*, 893–903. [[CrossRef](#)]

54. Gao, M.; Zhao, W.; Gong, Z.; Chen, Z.; Tang, X. Topographic correction of ZY-3 satellite images and its effects on estimation of shrub leaf biomass in mountainous areas. *Remote Sens.* **2014**, *6*, 3141–3151. [[CrossRef](#)]
55. Reese, H.; Olsson, H. C-correction of optical satellite data over alpine vegetation areas: A comparison of sampling strategies for determining the empirical c-parameter. *Remote Sens. Environ.* **2011**, *115*, 1387–1400. [[CrossRef](#)]
56. Sola, I.; González-Audícana, M.; Álvarez-Mozos, J. Multi-criteria evaluation of topographic correction methods. *Remote Sens. Environ.* **2011**, *184*, 247–262. [[CrossRef](#)]
57. Karathanassi, V.; Kolokousis, P.; Ioannidou, S. A comparison study on fusion methods using evaluation indicators. *Int. J. Remote Sens.* **2007**, *28*, 2309–2341. [[CrossRef](#)]
58. Zhang, J. Multi-source remote sensing data fusion: Status and trends. *Int. J. Image Data Fusion* **2010**, *1*, 5–24. [[CrossRef](#)]
59. Ni, W.; Sun, G.; Ranson, K.J.; Pang, Y.; Zhang, Z.; Yao, W. Extraction of ground surface elevation from ZY-3 winter stereo imagery over deciduous forested areas. *Remote Sens. Environ.* **2015**, *159*, 194–202. [[CrossRef](#)]
60. Hirano, A.; Welch, R.; Lang, H. Mapping from ASTER stereo image data: DEM validation and accuracy assessment. *ISPRS J. Photogramm.* **2003**, *57*, 356–370. [[CrossRef](#)]
61. Sefercik, U.G.; Alkan, M.; Buyuksalih, G.; Jacobsen, K. Generation and validation of high-resolution DEMs from Worldview-2 stereo data. *Photogramm. Rec.* **2013**, *28*, 362–374. [[CrossRef](#)]
62. Krishnan, S.; Sajikumar, N.; Sumam, K.S. DEM generation using Cartosat-I stereo data and its comparison with publically available DEM. *Procedia Technol.* **2016**, *24*, 295–302. [[CrossRef](#)]
63. Lu, D.; Mausel, P.; Batistella, M.; Moran, E. Comparison of land-cover classification methods in the Brazilian Amazon Basin. *Photogramm. Eng. Remote Sens.* **2004**, *70*, 723–732. [[CrossRef](#)]
64. Li, G.; Lu, D.; Moran, E.; Sant’Anna, S.J.S. A comparative analysis of classification algorithms and multiple sensor data for land use/land cover classification in the Brazilian Amazon. *J. Appl. Remote Sens.* **2012**, *6*, 061706. [[CrossRef](#)]
65. Bannari, A.; Morin, D.; Bonn, F.; Huete, A.R. A review of vegetation indices. *Remote Sens. Rev.* **1995**, *13*, 95–120. [[CrossRef](#)]
66. Baugh, W.M.; Groeneveld, D.P. Broadband vegetation index performance evaluated for a low-cover environment. *Int. J. Remote Sens.* **2006**, *27*, 4715–4730. [[CrossRef](#)]
67. Louhaichi, M.; Borman, M.; Johnson, D. Spatially located platform and aerial photography for documentation of grazing impacts on wheat. *Geocarto Int.* **2001**, *16*, 65–70. [[CrossRef](#)]
68. Wang, X.; Wang, M.; Wang, S.; Wu, Y. Extraction of vegetation information from visible unmanned aerial vehicle images. *Trans. Chin. Soc. Agric. Eng.* **2015**, *31*, 152–159. [[CrossRef](#)]
69. Haralick, R.M.; Shanmugam, K.; Dinstein, I.H. Textural features for image classification. *IEEE Trans. Syst. Man Cycle* **1973**, *3*, 610–621. [[CrossRef](#)]
70. Yu, Q.; Gong, P.; Clinton, N.; Biging, G.; Kelly, M.; Schirokauer, D. Object-based detailed vegetation classification with airborne high spatial resolution remote sensing imagery. *Photogramm. Eng. Remote Sens.* **2006**, *72*, 799–811. [[CrossRef](#)]
71. Jiao, L.; Liu, Y.; Li, H. Characterizing land-use classes in remote sensing imagery by shape metrics. *ISPRS J. Photogramm.* **2012**, *72*, 46–55. [[CrossRef](#)]
72. Fassnacht, F.E.; Latifi, H.; Sterenczak, K.; Modzelewska, A.; Lefsky, M.; Waser, L.T.; Straub, C.; Ghosh, A. Review of studies on tree species classification from remotely sensed data. *Remote Sens. Environ.* **2016**, *186*, 64–87. [[CrossRef](#)]
73. Keuchel, J.; Naumann, S.; Heiler, M.; Siegmund, A. Automatic land cover analysis for Tenerife by supervised classification using remotely sensed data. *Remote Sens. Environ.* **2003**, *86*, 530–541. [[CrossRef](#)]
74. Tso, B.; Mather, P.M. *Classification Methods for Remotely Sensed Data*; Taylor and Francis Inc.: New York, NY, USA, 2001.
75. Kimes, D.S.; Nelson, R.F.; Manry, M.T.; Fung, A.K. Attributes of neural networks for extracting continuous vegetation variables from optical and radar measurements. *Int. J. Remote Sens.* **1998**, *19*, 2639–2663. [[CrossRef](#)]
76. Gong, P.; Pu, R.; Yu, B. Conifer species recognition: An exploratory analysis of in situ hyperspectral data. *Remote Sens. Environ.* **1997**, *62*, 189–200. [[CrossRef](#)]
77. Cortijo, F.J.; Blanca, P.D.L. A comparative study of some non-parametric spectral classifiers. Applications to problems with high-overlapping training sets. *Int. J. Remote Sens.* **1997**, *18*, 1259–1275. [[CrossRef](#)]
78. Collions, M.J.; Dymond, C.; Johnson, E.A. Mapping subalpine forest types using networks of nearest neighbor classifiers. *Int. J. Remote Sens.* **2004**, *25*, 1701–1721. [[CrossRef](#)]
79. Haapanen, R.; Ek, A.R.; Bauer, M.E.; Finley, A.O. Delineation of forest/nonforest land use classes using nearest neighbor methods. *Remote Sens. Environ.* **2004**, *89*, 265–271. [[CrossRef](#)]

80. Lu, D.; Li, G.; Moran, E.; Kuang, W. A comparative analysis of approaches for successional vegetation classification in the Brazilian Amazon. *Gisci. Remote Sens.* **2014**, *51*, 695–709. [[CrossRef](#)]
81. Quinlan, J.R. Induction of Decision Trees. *Mach. Learn.* **1986**, *1*, 81–106. [[CrossRef](#)]
82. Landgrebe, D. A survey of decision tree classifier methodology. *IEEE Trans. Syst. Man Cycle* **1991**, *21*, 660–674. [[CrossRef](#)]
83. Friedl, M.A.; Brodley, C.E. Decision tree classification of land cover from remotely sensed data. *Remote Sens. Environ.* **1997**, *61*, 399–409. [[CrossRef](#)]
84. Osei-Bryson, K.M. Post-pruning in decision tree induction using multiple performance measures. *Comput. Oper. Res.* **2007**, *34*, 3331–3345. [[CrossRef](#)]
85. Fürnkranz, J. Pruning algorithms for rule learning. *Mach. Learn.* **1997**, *27*, 139–172. [[CrossRef](#)]
86. Hansen, M.; Dubayah, R.; DeFries, R. Classification trees: An alternative to traditional land cover classifiers. *Int. J. Remote Sens.* **1996**, *17*, 1075–1081. [[CrossRef](#)]
87. Lawrence, R.; Bunn, A.; Powell, S.; Zambon, M. Classification of remotely sensed imagery using stochastic gradient boosting as a refinement of classification tree analysis. *Remote Sens. Environ.* **2004**, *90*, 331–336. [[CrossRef](#)]
88. Breiman, L. Bagging predictors. *Mach. Learn.* **1996**, *24*, 123–140. [[CrossRef](#)]
89. Breiman, L. Random Forests. *Mach. Learn.* **2001**, *45*, 5–32. [[CrossRef](#)]
90. Stumpf, A.; Kerle, N. Object-oriented mapping of landslides using Random Forests. *Remote Sens. Environ.* **2011**, *115*, 2564–2577. [[CrossRef](#)]
91. Brown, M.; Gunn, S.R.; Lewis, H.G. Support vector machines for optimal classification and spectral unmixing. *Ecol. Model.* **1999**, *120*, 167–179. [[CrossRef](#)]
92. Wang, S.; Meng, B. Parameter selection algorithm for support vector machine. *Procedia Environ. Sci.* **2011**, *11*, 538–544. [[CrossRef](#)]
93. Hearst, M.A.; Dumais, S.T.; Osuna, E.; Platt, J.; Scholkopf, B. Support vector machines. *IEEE Intell. Syst. Their Appl.* **1998**, *13*, 18–28. [[CrossRef](#)]
94. Breerton, R.G.; Lloyd, G.R. Support vector machines for classification and regression. *Analyst* **2010**, *135*, 230–267. [[CrossRef](#)]
95. Foody, G.M. Status of land cover classification accuracy assessment. *Remote Sens. Environ.* **2002**, *80*, 185–201. [[CrossRef](#)]
96. Congalton, R.G.; Green, K. *Assessing the Accuracy of Remotely Sensed Data: Principles and Practices*, 2nd ed.; CRC Press: Boca Raton, FL, USA, 2008.
97. Liu, C.; Frazier, P.; Kumar, L. Comparative assessment of the measures of thematic classification accuracy. *Remote Sens. Environ.* **2007**, *107*, 606–616. [[CrossRef](#)]
98. Liu, Q.J.; Takamura, T.; Takeuchi, N.; Shao, G. Mapping of boreal vegetation of a temperate mountain in China by multitemporal Landsat TM imagery. *Int. J. Remote Sens.* **2002**, *23*, 3385–3405. [[CrossRef](#)]
99. Cho, M.A.; Mathieu, R.; Asner, G.P.; Naidoo, L.; Aardt, J.; Ramoelo, A.; Debba, P.; Wessels, K.; Main, R.; Smit, I.P.J.; et al. Mapping tree species composition in South African savannas using an integrated airborne spectral and LiDAR system. *Remote Sens. Environ.* **2012**, *125*, 214–226. [[CrossRef](#)]
100. Franklin, S.E.; Hall, R.J.; Moskal, L.M.; Maudie, A.J.; Lavigne, M.B. Incorporating texture into classification of forest species composition from airborne multispectral images. *Int. J. Remote Sens.* **2000**, *21*, 61–79. [[CrossRef](#)]
101. Wessel, M.; Brandmeier, M.; Tiede, D. Evaluation of different machine learning algorithms for scalable classification of tree types and tree species based on Sentinel-2 data. *Remote Sens.* **2018**, *10*, 1419. [[CrossRef](#)]
102. Blaschke, T.; Burnett, C.; Pekkarinen, A. Image segmentation methods for object-based analysis and classification. In *Remote Sensing Image Analysis: Including the Spatial Domain*; de Jong, S.M., van der Meer, F.D., Eds.; Kluwer Academic Publishers: Dordrecht, The Netherlands, 2004; pp. 211–236.
103. Myint, S.W.; Gober, P.; Brazel, A.; Grossman-Clarke, S.; Weng, Q. Per-pixel vs object-based classification of urban land cover extraction using high spatial resolution imagery. *Remote Sens. Environ.* **2011**, *115*, 1145–1161. [[CrossRef](#)]
104. Wang, D.; Wan, B.; Qiu, P.; Su, Y.; Guo, Q.; Wu, X. Artificial mangrove species mapping using Pléiades-1: An evaluation of pixel-based and object-based classifications with selected machine learning algorithms. *Remote Sens.* **2018**, *10*, 294. [[CrossRef](#)]

105. Gao, Y.; Mas, J.F.; Maathuis, B.H.P.; Zhang, X.; Van Dijk, P.M. Comparison of pixel-based and object-oriented image classification approaches—A case study in a Coal Fire Area, Wuda, Inner Mongolia, China. *Int. J. Remote Sens.* **2006**, *27*, 4039–4055. [[CrossRef](#)]
106. Zhang, C.; Xie, Z. Combining object-based texture measures with a neural network for vegetation mapping in the everglades from hyperspectral imagery. *Remote Sens. Environ.* **2012**, *124*, 310–320. [[CrossRef](#)]
107. Han, N.; Du, H.; Zhou, G.; Sun, X.; Ge, H.; Xu, X. Object-based classification using SPOT-5 imagery for Moso bamboo forest mapping. *Int. J. Remote Sens.* **2014**, *35*, 1126–1142. [[CrossRef](#)]



© 2019 by the authors. Licensee MDPI, Basel, Switzerland. This article is an open access article distributed under the terms and conditions of the Creative Commons Attribution (CC BY) license (<http://creativecommons.org/licenses/by/4.0/>).